Article

Juxtacrine Signaling Is Inherently Noisy

Tomer Yaron,[1] Yossi Cordova,[1,2] and David Sprinzak[1,*]
[1]Department of Biochemistry and Molecular Biology, Faculty of Life Sciences, Tel-Aviv University, Tel Aviv, Israel; and [2]Hemda Center for Science Education, 7 Ha Pardes St., Tel Aviv, Israel

ABSTRACT Juxtacrine signaling is an important class of signaling systems that plays a crucial role in various developmental processes ranging from coordination of differentiation between neighboring cells to guiding axon growth during neurogenesis. Such signaling systems rely on the interaction between receptors on one cell and trans-membrane ligands on the membrane of a neighboring cell. Like other signaling systems, the ability of signal-receiving cells to accurately determine the concentration of ligands, is affected by stochastic diffusion processes. However, it is not clear how restriction of ligand movement to the two-dimensional (2D) cell membrane in juxtacrine signaling affects the accuracy of ligand sensing. In this study, we use a statistical mechanics approach, to show that long integration times, from around one second to several hours, are required to reach high-sensing accuracy (better than 10%). Surprisingly, the accuracy of sensing cannot be significantly improved, neither by increasing the number of receptors above three to five receptors per contact area, nor by increasing the contact area between cells. We show that these results impose stringent constraints on the dynamics of processes relying on juxtacrine signaling systems, such as axon guidance mediated by Ephrins and developmental patterns mediated by the Notch pathway.

INTRODUCTION

Noise is a fundamental property of biological systems that affects biological functions ranging from transcriptional processes and chemotactic behavior at the single cell level to tissue development at the organismal level (1). Although many biological systems have to find ways to deal with noise to function reproducibly, other systems use noise for generating random processes or bet hedging strategies (2). One source of noise is the inherently stochastic behavior attributable to random diffusion of molecules in the environment. Such a diffusion driven noise, limits the accuracy at which the concentration of the ligand can be measured by cell surface receptors. This problem was first addressed by Berg and Purcell in 1977, who estimated the statistical fluctuations in ligand concentration and its effect on the accuracy of measurement by the cell (3). They showed that ligand diffusion introduces a counting error at the receptors, setting a noise floor for measuring ligand concentration. Based on the probability of a receptor to be occupied, they computed the fluctuation in receptor occupancy. Finally, relating the fluctuation in receptor occupancy with the uncertainty in ligand concentration at equilibrium, they obtained the relative uncertainty in the determination of the ligand concentration. This computation was also generalized for a system of many receptors.

A different approach using statistical mechanics and the fluctuation dissipation theorem was used to generalize the results of Berg and Purcell to a broader range of cases (4–6). This approach was based on using the fluctuations in receptor occupancy as a form of thermal noise, which allows using the fluctuation dissipation theorem rather than considering the microscopic details of the receptor-ligand interactions. They were able to separate noise coming from the binding/unbinding from the noise due to the ligand diffusion. The noise floor attributable to diffusion coincides with the results obtained by Berg and Purcell.

These methods provided an expression for the accuracy of the determination of ligand concentration, $\delta c/\overline{c}$, given an average ligand concentration, $\overline{c}$. For one receptor and for ligands diffusing in three dimensions (3D), the accuracy attributable to random diffusion of ligands is given by the following (3,4):

$$\frac{\delta c}{\overline{c}} \approx \frac{1}{\sqrt{\pi D_3 \overline{c} \tau a}}, \quad (1)$$

where D_3 is the ligand diffusion coefficient in 3D, τ is the measurement integration time, and a is the radius of the receptor.

It was also shown that increasing the number of receptors, m, which are used for sensing ligands, improves the accuracy. This improvement in accuracy is proportional to $1/\sqrt{m}$ at low m, but reaches saturation for high values of m. This saturation of the accuracy occurs because at some level no additional information is provided by adding more receptors, given a finite cell size (or finite size of receptor cluster).

Later works extended the analysis to include more detailed or cooperative ligand-receptor interactions (7–12),

Submitted March 25, 2014, and accepted for publication October 1, 2014.

*Correspondence: davidsp@post.tau.ac.il

Tomer Yaron and Yossi Cordova contributed equally to this work.

Editor: Stanislav Shvartsman.

0006-3495/14/11/2417/8 $2.00

http://dx.doi.org/10.1016/j.bpj.2014.10.006

lateral diffusion of receptors on the membrane (5), endocytosis of bound receptor-ligand pairs (6), and combined 3D and one dimensional (1D) diffusion for the case of transcription factors binding to DNA (13). The analysis was applied to several biological sensing processes including bacterial chemotaxis, intracellular signaling in *Escherichia coli* (*E. coli*), regulation by transcription factors, dynamics of flagellar motors, and neurotransmission in neural synapses (4,5).

In this study, we consider the effect of noise in an important class of signaling systems, termed juxtacrine signaling systems, in which the receptors on the membrane of one cell interact with ligands diffusing along the membrane of a neighboring cell (Fig. 1). Examples for such systems include the Notch signaling pathway, ephrins, semaphorins, and T-cell receptor-antigen interactions (14–17). The main difference between these systems and the systems considered previously is that both receptors and ligands diffuse in two dimensions (2D).

We show that the accuracy of sensing in 2D exhibits a very weak, logarithmic, dependence on the relevant length scales of the system. As a result of this weak dependence, the accuracy of ligand sensing is not significantly improved by having more than three to five receptors on the contact area between cells. Furthermore, increasing the contact area itself does not improve the accuracy either. We show that relatively long integration times, from around one second to several hours are required to reach accuracy of better than 10% (compared to milliseconds in typical 3D signaling systems). We discuss the implications of these results for biological processes relying on juxtacrine signaling systems, such as lateral inhibition and boundary formation mediated by the Notch signaling pathway and axon guidance mediated by cues from the ephrin signaling pathway.

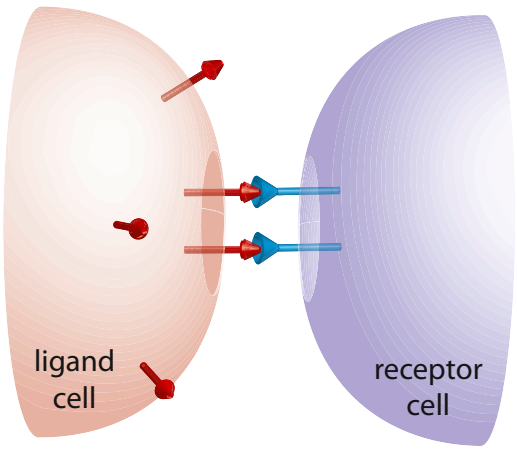

FIGURE 1 Schematic representation of a juxtacrine signaling system. We consider a geometry in which receptors on one cell (*blue symbols in right cell*) interact with ligands diffusing on the membrane of a neighboring cell (*red symbols in the left cell*). Ligands are assumed to diffuse freely on the membrane of the ligand cell and interact with receptors located at the contact area between the cells.

METHODS

Calculation of ligand concentration fluctuations in the 2D case

In our analysis, we consider one cell that expresses receptors (receptor cell) that comes in contact with a cell that expresses membrane-bound ligands (ligand cell, Fig. 1). We assume that the contact area is small compared with the total surface area of the cell membrane. We assume that the concentration of receptors is much smaller than that of the ligands, so that the receptors can be considered in terms of a discrete variable whereas the ligands are considered as continuous concentration. In the opposite case, where there are few ligands and many receptors, the ligands can be treated as a discrete variable and the receptors as a continuous concentration. The calculation of fluctuations in both cases is equivalent with the exception that the variables for receptors and ligands are exchanged. The special case where the concentrations of receptors and ligands are similar is not considered here.

We define the ligand concentration on the membrane of the ligand cell by $c(x,t)$. We also assume that ligands are continuously recycled in and out of the membrane uniformly (e.g., through endocytosis and exocytosis (18,19)) with rates k_{endo} and k_{exo}, respectively. The pursuing ligand dynamics is dictated by the following diffusion equation:

$$\frac{\partial c(\boldsymbol{x},t)}{\partial t} + \nabla \cdot j = -k_{endo}c(\boldsymbol{x},t) + k_{exo}c_{cyto}, \qquad (2)$$

where j is the ligands diffusion current on the cell membrane and to first order can be written as $j = -D_2\nabla c$, with D_2 being the 2D diffusion coefficient for the ligands on the cell membrane. c_{cyto} is the concentration of a cytoplasmic pool of the ligands that is assumed to be constant in this study. Given our assumption that the cell area is much larger than the contact area, we impose boundary conditions such that the concentration far from the contact is equal to the average concentration, namely, $c(\infty,t) = \overline{c} = k_{exo}c_{cyto}/k_{endo}$.

Following standard procedure in statistical mechanics (20), we add noise to the system by assuming a random perturbation in the chemical potential (see Supporting Material for detailed derivation). We allow a small perturbation, $\delta c^*(\boldsymbol{x},t)$, around the mean ligand concentration, $\overline{c}$ such that $c = \overline{c} + \delta c^*$ and calculate the power spectrum of δc^* defined by the following:

$$S(\omega,\boldsymbol{k}) \equiv \langle \delta c^*(\omega,\boldsymbol{k})\delta c^*(-\omega,-\boldsymbol{k})\rangle. \qquad (3)$$

Here, $\langle\ldots\rangle$ represents an ensemble average and $\delta c^*(\omega,\boldsymbol{k})$ is a Fourier transform of $\delta c^*(\boldsymbol{x},t)$ over all temporal and spatial frequencies ω and $\boldsymbol{k}$:

$$\delta c^*(\omega,\boldsymbol{k}) = \int dt \int d^2x e^{i(-\boldsymbol{k}\cdot\boldsymbol{x}+\omega t)}\delta c^*(\boldsymbol{x},t). \qquad (4)$$

Performing the calculation for the 2D case, the expression for the power spectrum is given by the following:

$$S(\omega,\boldsymbol{k}) = \frac{2\overline{c}(D_2k^2 + k_{endo})}{\omega^2 + (D_2k^2 + k_{endo})^2}. \qquad (5)$$

Calculation of accuracy of measurement by a single receptor

Next, we consider a single receptor that can measure ligand concentration in a radius roughly equivalent to its size, a, over an integration time, τ. We take the limit where the ligands that arrive at the receptors bind and are immediately released. This limit corresponds to the perfect monitoring disk approximation where the receptor simply counts the number of ligands diffusing through an area a (3,21). The effect of finite binding and unbinding has been previously taken into account (for the 3D case) and only

reduces the accuracy of measurement (3,4). The average ligand concentration measured by a receptor will be given by the following:

$$\tilde{c}(t,\boldsymbol{x}) = \int d^2x'dt' \; w_r(\boldsymbol{x}-\boldsymbol{x}')k_r(t-t')c(t',\boldsymbol{x}'), \quad (6)$$

where the function $w_r(\boldsymbol{x}-\boldsymbol{x}')$ defines the receptor spatial distribution and $k_r(t-t')$ defines the receptor temporal response. We choose Gaussian distribution profiles for $w_r(\boldsymbol{x}-\boldsymbol{x}')$ and $k_r(t-t')$ with standard deviations of a and τ, respectively. We then calculate the fluctuations measured by the receptor using (see Supporting Material) the following:

$$\langle \delta\tilde{c}(t,\boldsymbol{x})\delta\tilde{c}(t,\boldsymbol{x})\rangle = \int \frac{d\omega d^2k}{(2\pi)^3} S(\omega,\boldsymbol{k}) e^{-\tau^2\omega^2} e^{-a^2k^2} \quad (7)$$

The accuracy of measurement of ligand concentration by a single receptor can now be defined as $\delta c/\bar{c} \equiv \sqrt{\langle \delta\tilde{c}^2\rangle}/\bar{c}$.

Performing the integration in Eq. 7 we obtain an expression for the accuracy (see Supporting Material) that can be approximated by the following:

$$\frac{\delta c}{\bar{c}} \approx \frac{1}{\sqrt{\pi D_2 \bar{c}\tau}} \sqrt{\ln\left(\frac{\lambda}{a}\right)}, \quad (8)$$

where, λ, is the diffusion length scale of the ligand on the cell membrane. If the integration time is longer than the typical endocytosis time, namely when $\tau \gg k_{endo}^{-1}$, then the diffusion length scale is defined by $\lambda \equiv \sqrt{D_2/k_{endo}}$. In the opposite limit, if the integration time is shorter than the typical endocytosis time, namely when $\tau \ll k_{endo}^{-1}$, then the diffusion length scale is defined by $\lambda^* \equiv \sqrt{D_2\tau}$. Equation 8 is valid for $\lambda, \lambda^* \gg a$, which is typically the case because both λ and λ^* are expected to be of the order of few microns (based on typical diffusion constants, exchange rates, and integration times—see Table 1 (22–30)) and a is ~ 1 to 10 nm for typical receptors.

Calculation of accuracy of measurement by multiple receptors

Now we consider m receptors located on the contact surface between the cells (Fig. 1). Ligands are assumed to diffuse freely in 2D and are measured by the receptors at the contact area. We neglect for simplicity receptor diffusion, the effect of receptor internalization upon ligand binding, and cooperative effects in receptor-ligand binding (5–7,9).

To take into account the presence of m multiple receptors with radius a, we assume similarly to the case of one receptor that

$$\delta\tilde{c}(t,\boldsymbol{x}) = \sum\nolimits_{\mu=1}^{m} \int d^2x'dt' \; w_r(\boldsymbol{x}_\mu-\boldsymbol{x}')k_r(t-t')\delta c^*(t',\boldsymbol{x}'), \quad (9)$$

where $\boldsymbol{x}_\mu$ is the position of the μ-receptor. Eq. 7 then becomes the following:

$$\langle \delta\tilde{c}(t,\boldsymbol{x})\delta\tilde{c}(t,\boldsymbol{x})\rangle = \sum_{\mu,\nu} \int d\omega \frac{d^2k}{(2\pi)^3} e^{-\tau^2\omega^2} e^{-a^2k^2} \left(\frac{1}{m}\right) \times e^{i\boldsymbol{k}\cdot\boldsymbol{x}_\mu} \left(\frac{1}{m}\right) e^{-i\boldsymbol{k}\cdot x_\nu} \frac{2\bar{c}(D_2k^2+k_{endo})}{\omega^2+(D_2k^2+k_{endo})^2}. \quad (10)$$

Equation 10 can be estimated by taking the limit $\omega \approx 0$ (see Supporting Material):

$$\langle \delta\tilde{c}(t,\boldsymbol{x})\delta\tilde{c}(t,\boldsymbol{x})\rangle \approx \sum_{\mu\neq\nu} \left(\frac{1}{m^2}\right) \frac{\bar{c}}{\tau D_2\pi} K_0\left(\frac{|\boldsymbol{x}_\mu-\boldsymbol{x}_\nu|}{\lambda}\right) + \frac{\bar{c}}{\pi D_2\tau m}\ln\left(\frac{\lambda}{a}\right), \quad (11)$$

where K_0 is the modified Bessel function (31).

We now assume that the m receptors are distributed uniformly along the circumference of a contact area with radius s (Here, we take the same assumption as (4) regarding the geometry involved). This assumption allows us to simplify Eq. 11. In this case we obtain the following:

$$\left(\frac{\delta c}{\bar{c}}\right)^2 \approx \frac{1}{\pi D_2\bar{c}\tau m}\left[\ln\left(\frac{\lambda}{a}\right) + \sum\nolimits_{i=1}^{m-1} K_0\left(\frac{2s}{\lambda}\sin\left(\frac{\pi i}{m}\right)\right)\right] \quad (12)$$

In the limiting case where $\lambda \gg s$ we can use the asymptotic expansion for the modified Bessel function K_0 (31) to obtain the accuracy of ligand measurement by multiple receptors:

$$\frac{\delta c}{\bar{c}} \approx \frac{1}{\sqrt{\pi D_2\bar{c}\tau}} \sqrt{\frac{\ln\left(\frac{\lambda}{ma}\right)}{m} + \left(\frac{m-1}{m}\right)\ln\left(1.1228\,\frac{\lambda}{s}\right)}. \quad (13)$$

TABLE 1 Summary of typical biological parameters and estimated integration times to reach accuracy of 10% in measuring ligand concentration

Parameter	Value	Reference
D_2	0.01 to 0.1 $\mu m^2/s$	(22,23)
k_{endo}	0.001 to 0.01 1/s	(24–27)
C	1 to 100 μm^{-2}	(22,28–30)
S	0.1 to 5 μm	Small range corresponds to filopodia, large range corresponds to epithelial contacts.
$\tau_{min}\left(to\ reach \frac{\delta c}{c} = 0.1\right)$	0.91 s*	Calculated based on Eq. 12
$\tau_{max}\left(to\ reach \frac{\delta c}{c} = 0.1\right)$	3.22 h**	Calculated based on Eq. 13
$\tau_{3D,\ typical}\left(to\ reach \frac{\delta c}{c} = 0.1\right)$	0.03 s ***	Calculated based on (4)

All quantities were calculated using the limit of large number of receptors.
*τ_{min} ~ 0.91 s is calculated by numerically solving the equation, $(\delta c/\bar{c})^2 = 1/\pi m D_2\tau\bar{c}[\ln(\lambda^*/a) + \sum_{i=1}^{m-1} K_0((2s/\lambda^*)\sin(\pi i/m))]$, and assuming the following parameters: $k_{endo} = 10^{-2}$ 1/s, $D_2 = 10^{-1}$ μm ^{2}/s, $\bar{c} = 100$ 1/μm ^{2}, $\delta c/\bar{c} = 0.1$, $s = 5$ μm, and $m = 20$.
**τ_{max} ~ 3.22 h is calculated by solving Eq. 13 with $\lambda = \sqrt{D_2/k_{endo}}$, and assuming the following parameters: $k_{endo} = 10^{-3}$ 1/s, $D_2 = 10^{-2}$ μm ^{2}/s, $\bar{c} = 1$ 1/μm ^{2}, $\delta c/\bar{c} = 0.1$, $s = 0.1$ μm, and $m = 20$. We note that in this limit solving the exact formula (Eq. 12) gives the same result.
***$\tau_{3D,\ typical}$ ~ 0.03 s is calculated using $\tau_{3D} \approx 1/2\pi D_3\bar{c}a(\delta c/\bar{c})^2$ (4) by assuming the following parameters: $D_3 = 10$ μm ^{2}/s, $\bar{c} = 100\ nM$, $a = 1$ μm.

Similar to the case of one receptor, λ is replaced by λ^* when $\tau \ll k_{endo}^{-1}$ (see Supporting Material).

In the Supporting Material we also provide the derivation of the results (Eqs. 8 and 13) using an alternative method based on the fluctuation dissipation theorem (4). As expected, the binding-unbinding kinetics introduce an additional term to the accuracy similar to the one described in the 3D case (4).

Calculation of accuracy in the limit of a perfect absorber

In the calculation above we have taken the assumption of a perfect monitoring disk where ligands are immediately released upon binding to the receptors. It is useful to consider the opposite limit of a perfect absorber where the ligands are immediately removed from the contact area, for example by cleavage and internalization of the receptor-ligand pair. We have calculated the accuracy of sensing for this case based on a simple argument initially discussed in (3). In this calculation we directly integrate Eq. 2 with an additional boundary condition $c(a, t>0) = 0$, to obtain the total current impinging on a disk with radius a. Assuming a Poisson distribution, the accuracy of sensing would simply be proportional to $1/\sqrt{N}$, where N is the total number of ligands arriving at the receptor during the integration time. The accuracy obtained for this case is given by the following (see Supporting Material):

$$\frac{\delta c}{\overline{c}} \approx \frac{1}{\sqrt{2\pi D_2 \overline{c} \tau}} \sqrt{\ln\left(\frac{\lambda}{a}\right)} \tag{14}$$

Hence, for the case of a perfect absorber, the accuracy improves by a factor of $\sqrt{2}$, compared with the case of a perfect monitoring disk (Eq. 8).

RESULTS

Accuracy of ligand measurement for the one receptor case

Using statistical mechanics formalism, we have first calculated the measurement accuracy of the 2D ligand concentration by a single receptor on the membrane of the receptor cell (Fig. 1). We show in the methods that the expression we get for the accuracy of measurement in this case is given by the following:

$$\frac{\delta c}{\overline{c}} \approx \frac{1}{\sqrt{\pi D_2 \overline{c} \tau}} \sqrt{\ln\left(\frac{\lambda}{a}\right)} \tag{15}$$

For short integration times ($\tau \ll k_{endo}^{-1}$), the diffusion length scale in Eq. 15, $\lambda = \sqrt{D_2/k_{endo}}$ is replaced by $\lambda^* = \sqrt{D_2 \tau}$. This result differs from the 3D accuracy (Eq. 1) in several important ways. First, the accuracy improves (i.e., $\delta c/\overline{c}$ decreases) in a logarithmic manner as the receptor radius grows. Such logarithmic dependence appears in other quantities related to diffusion in 2D (32). Furthermore, the accuracy now depends on the diffusion length scale in the system, λ (or λ^*), which is the typical length scale from which ligands can diffuse into the contact area before they endocytose (or during the measurement integration time). This logarithmic dependence means that the accuracy now depends very weakly on the relevant length scales of the system (apart from the standard dependence on the length scale associated with the integration time $\sqrt{D_2 \tau}$).

Accuracy improves very little with increasing number of receptors

One possible strategy to improve the accuracy is to add more receptors at the contact area between cells. The number of receptors that come in contact with the ligands in a neighboring cell depends on the concentration of receptors on the cell membrane and on the contact area between cells. We therefore calculated how the accuracy changes both with the total number of receptors, m, in the contact area and with the radius of the contact area, s.

The accuracy of ligand concentration measurement for the case of m receptors, located on the contact surface between the cells (Fig. 1) are given by Eq. 12 (exact solution valid for any $\lambda \gg a$) and Eq. 13 (approximated solution for $\lambda > s$). Fig. 2 *A* and *B* show the dependence of the accuracy, $\delta c/\overline{c}$, on the number of receptors, different contact diameters between cells, and different integration times. For relatively short integration time ($\tau = 30$ s, Fig. 2 *A*) we use Eq. 12 with λ^* instead of λ, and for relatively long integration times ($\tau = 600$ s, Fig. 2 *B*) we use Eq. 13. For the case of one receptor ($m = 1$) we consistently recover the expression given by Eq. 15. As expected, increasing the number of receptors, m, improves the accuracy (see Fig. 2 *A* and *B*) but, surprisingly, this improvement saturates when the number of receptors is greater than three to five receptors. The accuracy at saturation is simply the accuracy one would get if the whole contact area was considered to be one large receptor. Namely, for large m, Eq. 13 takes a similar form to the one receptor result (Eq. 15) but with the receptor radius, a, replaced by the radius of the contact area, s. Simple analysis of Eq. 13 shows that the saturation value, m_{sat}, depends on the ratio between two logarithms, $m_{sat} \cong 1 + (\ln(\lambda/a)/\ln(\lambda/s))$, and hence depends very weakly on all the relevant length scales in Eq. 13 (i.e., diffusion length scale, size of the receptor, and size of the contact area). The effect of adding more receptors is therefore much weaker in this 2D geometry compared with the 3D geometry, where this saturation is reached when $m_{sat} \cong 2s/a$ that can range from several hundreds to several thousands receptors (4). Longer integration times naturally improve the accuracy, but the weak dependence on the number of receptors, remains (Fig. 2 *B*). Hence, unlike the 3D case, the accuracy cannot be significantly improved by adding more receptors.

Accuracy improves very little with increasing contact area

It is interesting to ask whether the accuracy is affected by the contact area between cells. For a fixed concentration of receptors, increasing the contact area increases both m and s. Fig. 2 *C* and *D* show the dependence of the accuracy on contact radius for different receptor concentrations and different integration times. For typical values of ligand concentrations, the accuracy saturates when the contact radius

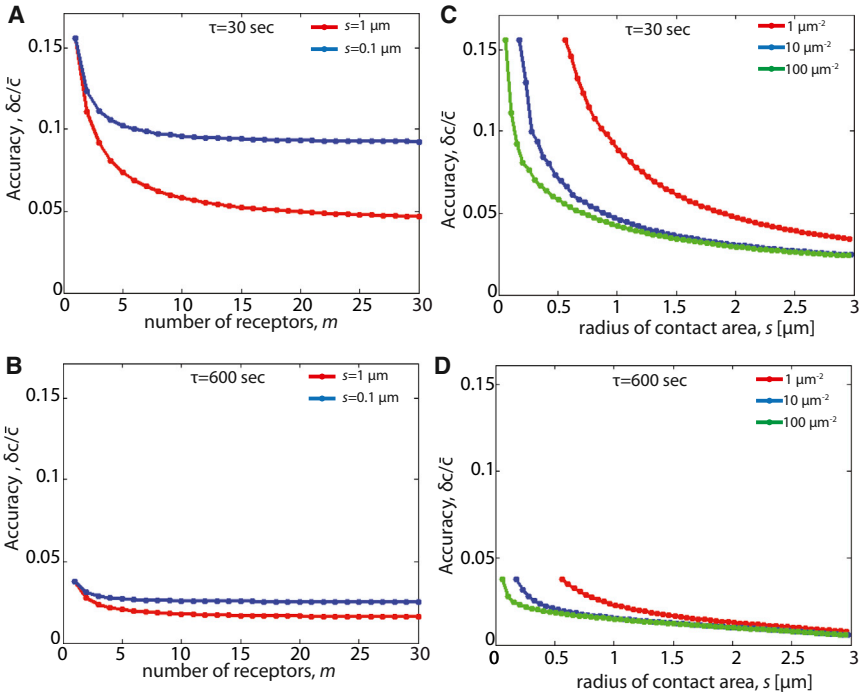

FIGURE 2 Dependence of measurement accuracy on number of receptors, contact area, and integration time. (*A–B*) Dependence of measurement accuracy of ligand concentration, $\delta c/\bar{c}$, on the number of receptors at the contact area, m, for relatively short integration time (*A*, $\tau = 30$ s) and for relatively long integration time (*B*, $\tau = 600$ s). The accuracy in all cases saturates at around three to five receptors. The accuracy is calculated using the exact solution, Eq. 12, for *A*, and the approximate solution, Eq. 13, for *B* (because the condition for approximation, $s<\lambda$, can only be applied in *B*). The following parameters are used: $D_2 = 0.03$ μm^2/s, $\bar{c} = 100$ molecules/μm^2, $K_{endo} = 3*10^{-3}$ 1/s, $a = 1$ nm, and the radius of the contact area, s, as indicated in the figure legend. Because in A $\tau<k_{endo}$, we use $\lambda^* = \sqrt{D_2\tau}$ instead of $\lambda = \sqrt{D_2/k_{endo}}$ for this case. (*C–D*) Dependence of measurement accuracy of ligand concentration, $\delta c/\bar{c}$, on the radius of the contact area, s, for relatively short integration time (*C*, $\tau = 30$ s) and for relatively long integration time (*D*, $\tau = 600$ s). The plot shows that the accuracy does not significantly improve when $s > 0.5$ to 1.5 μm. As in *A–B*, the accuracy is calculated using the exact solution, Eq. 12, for *A*, and the approximate solution, Eq. 13, for *B*. The number of receptors for each value of s was calculated using $m = \pi s^2 \sigma_R$, where σ_R is the receptor density. In the exact calculation m was rounded to the nearest integer number. $D_2 = 0.03$ μm^2/s, $\bar{c} = 100$ molecules/μm^2, $K_{endo} = 3*10^{-3}$ 1/s, $a = 1$ nm, σ_R as indicated in the figure legend. Comparison of the exact and approximate solutions is provided in Fig. S1.

is above a few microns, corresponding to the radius in which the number of receptors in the contact area reaches the saturation value, m_{sat}. Longer integration times (Fig. 2 *D*) improve the accuracy (compared with shorter integration time, Fig. 2 *C*) but show saturation at similar contact areas. As in the previous section, we use Eq. 12 with λ^* instead of λ for short integration times ($\tau = 30$ s, Fig. 2C), and Eq. 13 for relatively long integration times ($\tau = 600$ s, Fig. 2 *B*). We note that, the approximated solution in Eq. 13 works nicely for longer integration times but breaks down (as expected) in the limit of large contact radii and short integration time (Fig. S1). This result suggests that there is almost no advantage in terms of accuracy of measurement in having large contact area between cells.

Another way to understand this weak dependence of the accuracy on the number of receptors and the contact area is by realizing that diffusion in 2D is known to exhibit long-range density fluctuations (logarithmic dependence) (33). These long-range correlations limit the ability of the receptor cell to accurately determine the average ligand concentration even when the whole contact area can be treated as one effective receptor with large contact area.

Integration times of up to several hours are required to reach high accuracy

How long would it typically take for a receptor cell to accurately determine ligand concentration in a neighboring cell? Using Eqs. 12 and 13 (applied in different parameter regimes) we can estimate the typical time it would take to reach an accuracy of 10% ($\delta c/\bar{c} = 0.1$). For typical values of parameters, we find that cells may need to integrate between around 1 second to 3 hours (see Table 1). These are considerably longer times than the time it would take an eukaryotic cell to accurately measure the concentration of a ligand diffusing in 3D, which is typically in the millisecond range (see Table 1 and (5)). It is interesting to note, that developmental processes, in which juxtacrine signaling systems are being used, may occur over periods of time that are shorter than the typical integration times calculated above. It is therefore not clear how signaling can be accurately determined in these systems.

Averaging over several neighboring cells modestly improve accuracy

Cells in higher organisms typically come in contact with several neighboring cells, raising the question of how the accuracy of sensing changes when a receptor cell is in contact with multiple ligand cells. Assuming that the receptor cell integrates over the signal from all its neighbors and that fluctuations are uncorrelated between cells, it is easy to show that the accuracy improves modestly by a factor of $1/\sqrt{N}$, where N is the number of neighbors (see Supporting Material). For cells in an epithelial cell layer, which have six neighbors in average this would correspond to improving the accuracy by a factor of ~ 2.5.

Processing of receptor-ligand pair improves accuracy by a factor of up to $\sqrt{2}$

Some juxtacrine signaling systems undergo processing upon receptor-ligand binding; for example, the Notch receptor is cleaved once bound to its ligand and its extracellular domain trans-endocytose into the ligand expressing cell (34). Such processing prevents the unbinding of the ligand and the possibility of measuring the same ligand more than once (6). In the limit of very fast processing, namely, that processing rate is much faster than the unbinding rate, one can consider the receptor as a perfect absorber that counts and removes all the ligands impinging on it (3,21) (we assume each processed receptor is immediately replaced by a new one). The accuracy of measurement by a perfect absorber in the 3D case was previously shown to be better than the accuracy of a perfect monitoring sphere by a numerical factor (21). We perform a similar calculation for the accuracy of a perfect absorber for the 2D case, taking into account endocytosis and exocytosis. We show that the accuracy improves by a factor of $\sqrt{2}$ compared with the result in Eq. 8 (see Methods and Supporting Material). Note that, receptor-ligand processing may also reduce the accuracy if it takes time for the processed receptor to be replaced by a new one.

DISCUSSION

From the point of view of the receptor cell, there are two general strategies to improve accuracy of detection. One strategy is to integrate the signal over longer times. Although this strategy certainly improves accuracy it comes with a price: a longer integration time means a slower response time of the system. We show that for typical values of parameters, integration times ranging from around one second to 3 h are required to reach accuracy better than 10%. Many biological systems may be required to operate on faster time scales.

The second strategy is to improve detection by adding more receptors. This strategy seems to work well in 3D signaling systems, where the accuracy can be improved significantly by increasing the number of receptors. In this case, the improvement in accuracy reaches saturation when $m_{sat} \cong 2s/a$. For chemotactic receptors in *E. coli*, this threshold value may reach many hundreds of receptors (3,4). In contrast, the behavior of the accuracy in the 2D juxtacrine signaling system is dramatically different. Although adding additional receptors initially improves accuracy, it reaches saturation when $m_{sat} \cong 1 + (\ln(\lambda/a)/\ln(\lambda/s)) \cong 3 - 5$, for typical values of parameters (Fig. 2 *A* and *B*). Similarly, increasing the contact area between cells (Fig. 2 *C* and *D*) or averaging over signal from multiple neighbors does not significantly improve the accuracy. This result has striking implications on the ability of cells to sense signaling from their neighbors in an accurate manner.

Reduced accuracy imposes a constraint on speed of axon growth

What are the implications of these results on specific biological processes that rely on juxtacrine signaling? One such process is axon guidance, in which neurons send out axons to their correct targets during neural development (35). This process is mediated by juxtacrine signaling systems such as the ephrin signaling pathway (but also other signaling systems may be involved). Ephrins from the target cells interact with Eph receptors on the growth cone of the axon. The axons in this process often respond to gradients of ephrins expressed in the target tissue and stop growing when they reach specific ligand concentration (36) (see Fig. 3 *A*). Our results suggest that there may be a constraint on the

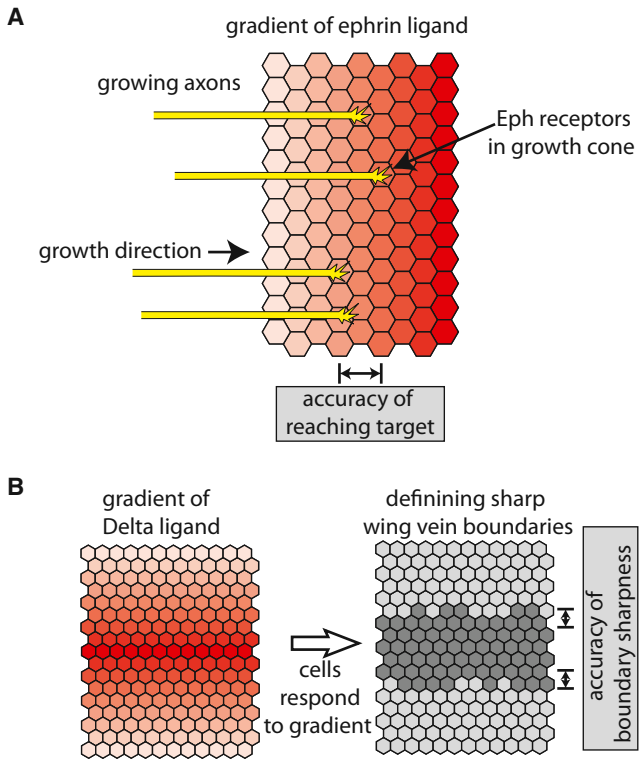

FIGURE 3 Implications of accuracy constraints on ephrin mediated axon guidance and Notch mediated patterning. (*A*) An illustration of axon guidance mediated by ephrin signaling. During axon development, axons (*yellow*) that express Eph receptors in their growth cones, grow into the target tissue that express a gradient of ephrin ligands (*red*). Eph signaling is used for the determination of target positions for the axons. The limit on accuracy of measurement in juxtacrine signaling imposes a constraint on the growth rate of axons. For example, assuming that 1 min integration time is required for reaching an accuracy enough to distinguish between ephrin concentration in neighboring cells (say 10% difference between cells that are 10 μm apart), imposes a limit on the growth rate of axons to 10 μm/min. (*B*) A simplified illustration of Notch mediated wing vein development in Drosophila. During wing vein formation, a gradient of Delta expression in the future vein region (*red*) is used for defining the boundary between vein (*dark gray*) and intervein (*light gray*) regions. Here, the limit on accuracy of measurement in juxtacrine signaling may impose a constraint on the developmental time required for achieving sharp boundaries (see text).

growth rate of the axons because the growing neurons may require long integration times to accurately determine the ephrin concentration in the target tissue. Assuming growing axons need to distinguish between ephrin concentrations that are ~ 10% different (37), presented on cells 10 μm in diameter, we estimate that the maximal growth rate of the axons for typical parameters (assuming 1 min integration time) should not exceed 10 μm/min. Interestingly, some axons have been shown to reach growth rates as fast as 5 μm/min (38,39), suggesting that growth rate may indeed be limited by the ability to accurately measure ephrin concentration during axon guidance.

Implications of result to Notch mediated patterning

Another example for processes that may be affected by our results are Notch mediated patterning processes. The Notch signaling pathway is involved in different developmental processes in which neighboring cells adopt different fates. For example, during wing development in *Drosophila melanogaster,* the Notch pathway is used in defining sharp vein boundaries (40,41). In this system, a gradient of Delta expression is converted into a sharp Notch signaling response that translates to a sharp boundary defined by an almost perfect 1D line of cells (Fig. 3 *B*). It has been shown that such a mechanism may be very sensitive to noise in Notch signaling (42). Although this process certainly involves more complex regulatory processes, it is useful to ask, in the context of a simple Notch readout model, what would be the typical integration time required to achieve such accurate patterning. Given that the concentration of Delta may vary by an estimated 10% to 20% over one cell diameter (estimated from (40)), we can estimate that achieving such spatial accuracy would require up to 10 min. Although the process of wing vein formation takes several hours, it is not clear at what stage during wing development are cell fates determined. It has been shown that target genes downstream of Notch signaling may exhibit transient response lasting only a few minutes (43), which may suggest that this process may also be limited by the time it takes to accurately determine Delta concentration along the gradient.

Notch is also involved in patterning processes in which small initial differences between cells are amplified to generate alternating salt-and-pepper differentiation patterns in a process termed lateral inhibition (44,45). It is possible that our finding that such signaling systems are inherently noisy may be useful in this context. Such noise may help generate large initial differences between cells that can help generating patterned states more quickly (42).

The conclusions discussed above rely on several simplifying assumptions including assuming that the receptors do not diffuse, that the concentrations of receptors and ligands are unmatched, and that the biochemical details of the signaling pathway such as clustering of receptors are neglected. The contribution of some of these effects has been addressed elsewhere for the 3D case and is beyond the scope of this study (5–7,9). Given that the source of noise for juxtacrine signaling is the long-range density fluctuations in 2D diffusion, we expect that the exact details of the biochemistry would not dramatically improve the accuracy of sensing. Similarly, we do not expect that the accuracy would be significantly improved for the special case where receptor and ligand concentrations are similar. Nevertheless, it would be interesting to explore the effect of receptor-ligand binding-unbinding on the accuracy in juxtacrine signaling as has been done in 3D systems (7–12).

Regarding the role of receptor diffusion, one way to look at this problem is to say that receptor diffusion effectively increases the diameter of the area probed by the receptor (a in Eq. 15). Because this diameter goes into the logarithmic term, we do not expect receptor diffusion to affect the uncertainty much. Nevertheless, it would be interesting to explore these effects in detail in the future. Finally, it will be interesting to consider the implications of our results on other developmental processes such as planar cell polarity and the immune system relying on different signaling pathways than the ones discussed in this study.

SUPPORTING MATERIAL

One figure and supplementary methods is available at http://www.biophysj.org/biophysj/supplemental/S0006-3495(14)01057-1.

We would like to acknowledge the help of Idse Heemskerk, Boris Shraiman, Pau Formosa Jordan, Oren Shaya, Menachem Gutman, and Avigdor Eldar for critically reviewing the manuscript and Avraham Yaron and Nir Friedman for helpful discussions.

This work was supported by grants from the Israeli Science Foundation (Grant No. 1021/11) and a Marie Curie European Reintegration Grant.

SUPPORTING CITATIONS

References (46–54) appear in the Supporting Material.

REFERENCES

1. Eldar, A., and M. B. Elowitz. 2010. Functional roles for noise in genetic circuits. *Nature.* 467:167–173.
2. Perkins, T. J., and P. S. Swain. 2009. Strategies for cellular decision-making. *Mol. Syst. Biol.* 5:326.
3. Berg, H. C., and E. M. Purcell. 1977. Physics of chemoreception. *Biophys. J.* 20:193–219.
4. Bialek, W., and S. Setayeshgar. 2005. Physical limits to biochemical signaling. *Proc. Natl. Acad. Sci. USA.* 102:10040–10045.
5. Aquino, G., and R. G. Endres. 2010. Increased accuracy of ligand sensing by receptor diffusion on cell surface. *Phys. Rev. E Stat. Nonlin. Soft Matter Phys.* 82:041902.
6. Aquino, G., and R. G. Endres. 2010. Increased accuracy of ligand sensing by receptor internalization. *Phys. Rev. E Stat. Nonlin. Soft Matter Phys.* 81:021909.

7. Endres, R. G., and N. S. Wingreen. 2006. Precise adaptation in bacterial chemotaxis through "assistance neighborhoods". *Proc. Natl. Acad. Sci. USA.* 103:13040–13044.
8. Skoge, M. L., R. G. Endres, and N. S. Wingreen. 2006. Receptor-receptor coupling in bacterial chemotaxis: evidence for strongly coupled clusters. *Biophys. J.* 90:4317–4326.
9. Skoge, M., Y. Meir, and N. S. Wingreen. 2011. Dynamics of cooperativity in chemical sensing among cell-surface receptors. *Phys. Rev. Lett.* 107:178101.
10. Bialek, W., and S. Setayeshgar. 2008. Cooperativity, sensitivity, and noise in biochemical signaling. *Phys. Rev. Lett.* 100:258101.
11. Wang, K., W. J. Rappel, …, H. Levine. 2007. Quantifying noise levels of intercellular signals. *Phys. Rev. E Stat. Nonlin. Soft Matter Phys.* 75:061905.
12. Berezhkovskii, A. M., and A. Szabo. 2013. Effect of ligand diffusion on occupancy fluctuations of cell-surface receptors. *J. Chem. Phys.* 139:121910.
13. Tkacik, G., and W. Bialek. 2009. Diffusion, dimensionality, and noise in transcriptional regulation. *Phys. Rev. E Stat. Nonlin. Soft Matter Phys.* 79:051901.
14. Artavanis-Tsakonas, S., M. D. Rand, and R. J. Lake. 1999. Notch signaling: cell fate control and signal integration in development. *Science.* 284:770–776.
15. Klein, R. 2004. Eph/ephrin signaling in morphogenesis, neural development and plasticity. *Curr. Opin. Cell Biol.* 16:580–589.
16. Tamagnone, L., S. Artigiani, …, P. M. Comoglio. 1999. Plexins are a large family of receptors for transmembrane, secreted, and GPI-anchored semaphorins in vertebrates. *Cell.* 99:71–80.
17. Cemerski, S., and A. Shaw. 2006. Immune synapses in T-cell activation. *Curr. Opin. Immunol.* 18:298–304.
18. Battey, N. H., N. C. James, …, C. Brownlee. 1999. Exocytosis and endocytosis. *Plant Cell.* 11:643–660.
19. Maxfield, F. R., and T. E. McGraw. 2004. Endocytic recycling. *Nat. Rev. Mol. Cell Biol.* 5:121–132.
20. Chaikin, P. M., and T. C. Lubensky. 1995. Principles of Condensed Matter Physics. Cambridge University Press, New York.
21. Endres, R. G., and N. S. Wingreen. 2008. Accuracy of direct gradient sensing by single cells. *Proc. Natl. Acad. Sci. USA.* 105:15749–15754.
22. McCloskey, M. A., and M. M. Poo. 1986. Rates of membrane-associated reactions: reduction of dimensionality revisited. *J. Cell Biol.* 102:88–96.
23. Bray, S., and F. Bernard. 2010. Notch targets and their regulation. *Curr. Top. Dev. Biol.* 92:253–275.
24. Wiley, H. S., and D. D. Cunningham. 1982. The endocytotic rate constant. A cellular parameter for quantitating receptor-mediated endocytosis. *J. Biol. Chem.* 257:4222–4229.
25. Sorkin, A., and J. E. Duex. 2010. Quantitative analysis of endocytosis and turnover of epidermal growth factor (EGF) and EGF receptor. *Curr. Protoc. Cell Biol.* 15:14.
26. Felder, S., J. LaVin, …, J. Schlessinger. 1992. Kinetics of binding, endocytosis, and recycling of EGF receptor mutants. *J. Cell Biol.* 117:203–212.
27. Cole, N. B., and J. G. Donaldson. 2012. Releasable SNAP-tag probes for studying endocytosis and recycling. *ACS Chem. Biol.* 7:464–469.
28. Waters, C. M., K. C. Oberg, …, K. A. Overholser. 1990. Rate constants for binding, dissociation, and internalization of EGF: effect of receptor occupancy and ligand concentration. *Biochemistry.* 29:3563–3569.
29. Weinmaster, G., and J. A. Fischer. 2011. Notch ligand ubiquitylation: what is it good for? *Dev. Cell.* 21:134–144.
30. Shimizu, K., S. Chiba, …, H. Hirai. 1999. Mouse jagged1 physically interacts with notch2 and other notch receptors. Assessment by quantitative methods. *J. Biol. Chem.* 274:32961–32969.
31. Olver, F. W. J., D. W. Lozier, …, C. W. Clark. 2010. NIST Handbook of Mathematical Functions. Cambridge University Press, New York.
32. Adam, G., and M. Delbruck. 1968. Reduction of Dimensionality in Biological Diffusion Processes. W. H. Freeman & Co., New York.
33. Barton, G. 1989. Elements of Green Functions and Propagation Potentials, Diffusion and Waves. Oxford Science/Clarendon Press, Oxford, UK.
34. Kopan, R., and M. X. G. Ilagan. 2009. The canonical Notch signaling pathway: unfolding the activation mechanism. *Cell.* 137:216–233.
35. Tessier-Lavigne, M., and C. S. Goodman. 1996. The molecular biology of axon guidance. *Science.* 274:1123–1133.
36. Lang, S., A. C. von Philipsborn, …, M. Bastmeyer. 2008. Growth cone response to ephrin gradients produced by microfluidic networks. *Anal. Bioanal. Chem.* 390:809–816.
37. Higenell, V., S. M. Han, …, E. S. Ruthazer. 2012. Expression patterns of Ephs and ephrins throughout retinotectal development in Xenopus laevis. *Dev. Neurobiol.* 72:547–563.
38. Pfister, B. J., A. Iwata, …, D. H. Smith. 2004. Extreme stretch growth of integrated axons. *J. Neurosci.* 24:7978–7983.
39. Koo, B. K., H. S. Lim, …, Y. Y. Kong. 2005. Mind bomb 1 is essential for generating functional Notch ligands to activate Notch. *Development.* 132:3459–3470.
40. de Celis, J. F., S. Bray, and A. Garcia-Bellido. 1997. Notch signalling regulates veinlet expression and establishes boundaries between veins and interveins in the Drosophila wing. *Development.* 124:1919–1928.
41. Koo, B. K., K. J. Yoon, …, Y. Y. Kong. 2005. Mind bomb-2 is an E3 ligase for Notch ligand. *J. Biol. Chem.* 280:22335–22342.
42. Sprinzak, D., A. Lakhanpal, …, M. B. Elowitz. 2011. Mutual inactivation of Notch receptors and ligands facilitates developmental patterning. *PLOS Comput. Biol.* 7:e1002069.
43. Koo, B. K., M. J. Yoon, …, Y. Y. Kong. 2007. An obligatory role of mind bomb-1 in notch signaling of mammalian development. *PLoS ONE.* 2:e1221.
44. Heitzler, P., and P. Simpson. 1991. The choice of cell fate in the epidermis of Drosophila. *Cell.* 64:1083–1092.
45. Collier, J. R., N. A. Monk, …, J. H. Lewis. 1996. Pattern formation by lateral inhibition with feedback: a mathematical model of delta-notch intercellular signalling. *J. Theor. Biol.* 183:429–446.
46. Kubo, R. 1966. The fluctuation-dissipation theorem. *Rep. Prog. Phys.* 29:255–284.
47. Landau, L. D., and E. M. Lifshitz. 1980. Statistical Physics Part I. Pergamon Press, Oxford, UK.
48. Pathria, R. K. 1972. Statistical Mechanics. Pergamon Press, Oxford, UK.
49. Landau, L. D., and E. M. Lifshitz. 1980. Statistical Physics Part II. Pergamon Press, Oxford, UK.
50. Kanwal, R. P. 1983. Generalized Functions Theory and Technique. Mathematics in Science and Engineering, Vol. 171. Academic Press, New York.
51. Gelfand, I. M., and G. E. Shilov. 1964. Generalized Functions. Vol. 1. Properties and Operations. Academic Press, New York.
52. Morse, P. M., and H. Feshbach. 1953. Methods of Theoretical Physics, Vol. 1. McGraw-Hill, New York.
53. http://www.siam.org/journals/categories/05–001.php.
54. Goldstein, B., R. Griego, and C. Wofsy. 1984. Diffusion-limited forward rate constants in two dimensions. Application to the trapping of cell surface receptors by coated pits. *Biophys. J.* 46:573–586.

Juxtacrine signaling is inherently noisy

Supplementary information

Tomer Yaron[1*], Yossi Cordova[1,2*], and David Sprinzak[1]

1. Department of Biochemistry and Molecular Biology, Faculty of life sciences, Tel-Aviv University, Tel Aviv 69978, Israel
2. Hemda center for Science Education, 7 Ha Pardes st., Tel Aviv 6424534, Israel

* These authors contributed equally to the manuscript

Supplementary Figures

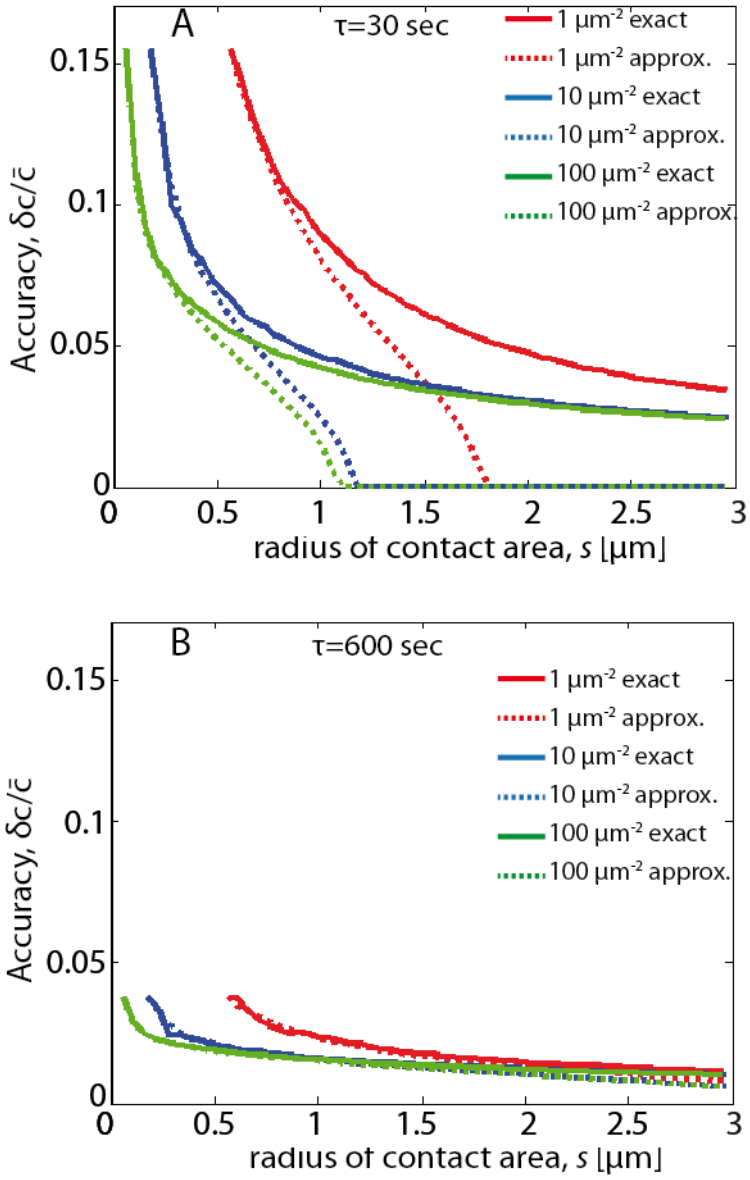

Figure S1: Comparison of exact and approximate solutions for the accuracy of measurement. (A,B) Dependence of measurement accuracy of ligand concentration, $\frac{\delta c}{\bar{c}}$, on the radius of the contact area, s, for relatively short integration time (A, τ=30 sec) and for relatively long integration time (B, τ=600 sec) calculated either with *Eq.* 12 (solid lines) or *Eq.* 13 (dashed lines). The plot shows that the approximate solution works well for long integration times (B) but breaks down for short integration times and large contact radii (A). This is since the condition $s < \lambda, \lambda^*$ no longer holds in this parameter regime. For these plots the same parameters as Fig. 2C,D were used.

Supplementary methods

The purpose of this supplementary information is to describe in detail, the calculation of the accuracy of measuring ligand concentration by one receptor and its extension to several receptors. The supplementary information is divided into four sections. In the first section we calculate the accuracy of ligand concentration measurement by one receptor acting as a perfect instrument ('perfect monitoring disk' approximation), assuming fluctuations induced by the diffusion of ligands. In the second section we extend the calculation of accuracy of ligand concentration to the case of several receptors. In the third section we present a detailed computation of the accuracy of ligand sensing by a perfect absorbing receptor. In the fourth section we present an alternative computation of the accuracy in measuring ligand concentration based on the fluctuation dissipation theorem (FDT) (1,2) and assuming intrinsic noise in the receptor-ligand system.

Accuracy of ligand concentration measurement by one receptor

The ligand concentration on the membrane of the ligand cell is described by $c(\boldsymbol{x},t)$. We assume that ligands are continuously recycled in and out of the membrane (e.g. through endocytosis and exocytosis with rates k_{endo} and k_{exo}, respectively. The dynamics of receptor-ligand interactions is dictated by

$$\frac{\partial c(\boldsymbol{x},t)}{\partial t} + \nabla \cdot j = -k_{endo} c(\boldsymbol{x},t) + k_{exo} c_{cyto} \text{ , (S1)}$$

where j is the ligands diffusion current on the cell membrane and to first order can be written as $j = -D_2 \nabla c$.

D_2 is the ligand diffusion coefficient. External noise is included by adding a current $j_d = -\gamma c \nabla \mu$, where γ is the ligand mobility and μ is the chemical potential. In thermodynamic equilibrium, the ligand concentration satisfies the Boltzman relation $\mu = k_B T ln c$, where k_B is the Boltzman constant and T represents the temperature. Therefore $\nabla \cdot (\beta D_2 c \nabla \mu + \gamma c \nabla \mu)$=0, where $\beta = \frac{1}{KT}$, leads to $\beta D_2 = \gamma$ (3).

Hence, in the presence of an external noise, Eq. S1 is replaced by

$$\frac{\partial c(\boldsymbol{x},t)}{\partial t} - D_2 \nabla^2 c = \beta D_2 \nabla (c \nabla \mu) - k_{endo} c(\boldsymbol{x},t) + k_{exo} c_{cyto} \text{ . (S2)}$$

Next we introduce a random noise in the chemical potential μ that satisfies

$$\langle \delta\mu(t,\boldsymbol{k}) \delta\mu(t',-\boldsymbol{k}) \rangle = A(k)\delta(t-t'), \text{ (S3)}$$

where $k = |\boldsymbol{k}|$. The notation $\langle \dots \rangle$ represents an ensemble average. The fluctuation in the chemical potential is defined by $\delta\mu = \mu - \bar{\mu}$, where $\bar{\mu}$ is the chemical

potential average value, and $\mu(t, \boldsymbol{k})$ is the spatial Fourier transform of the chemical potential. We define the Fourier transform in spatial and temporal variables of a function $f(\boldsymbol{x}, t)$ according to the following standard definition

$f(\omega, \boldsymbol{k})$=$\int dt \int d^2x\, e^{i(-\boldsymbol{k}\cdot\boldsymbol{x}+\omega t)} f(\boldsymbol{x}, t)$. (S4)

Similarly we define the fluctuations in the ligand concentration by δc^*, $c = \bar{c} + \delta c^*$, where $\bar{c}$ represents the ligand average concentration. Eq. S2 may be rewritten in terms of the fluctuations δc^* and $\delta\mu$ as

$\frac{\partial \delta c^*(\boldsymbol{x},t)}{\partial t} - D_2\nabla^2\delta c^* = \beta D_2 \bar{c}\, \nabla^2(\delta\mu) - k_{endo}\delta c^*(\boldsymbol{x}, t)$. (S5)

The Fourier transform of Eq. S5 in spatial and temporal variables leads to

$\delta c^*(\omega, \boldsymbol{k}) = \frac{-\beta \bar{c} D_2 k^2}{-i\omega + D_2 k^2 + k_{endo}} \delta\mu(\omega, \boldsymbol{k})$. (S6)

The next step is to compute the power spectrum of the fluctuation δc^*: $S_c(\omega, \boldsymbol{k}) = \langle \delta c^*(w, \boldsymbol{k}) \delta c^*(-\omega, -\boldsymbol{k}) \rangle$ (4). We calculate the power spectrum $S_c(\omega, \boldsymbol{k})$ using Eq. S3 and Eq. S6 obtaining

$S_c(\omega, \boldsymbol{k}) = \mathrm{A}\beta^2 \bar{c}^2 \frac{(D_2 k^2)^2}{\omega^2 + (D_2 k^2 + k_{endo})^2}$. (S7)

In the case of a solution at low concentration (ideal gas approximation) it is known that $\mu = \beta^{-1} ln\, c$, then applying the equipartition theorem (5) to the variable c and its conjugate $\mu = \frac{\partial E}{\partial c}$,we get $\langle \delta c^*(t) \delta\mu(t) \rangle = \beta^{-1} = \beta^{-1}\bar{c}^{-1}\langle \delta c^*(t)^2 \rangle$. Therefore (4)

$\langle \delta c^*(t)^2 \rangle$ =$\bar{c}$. (S8)

It is well known that the power spectrum satisfies (2)

$\langle \delta c^*(t)^2 \rangle = \int \frac{d\omega}{2\pi} S_c(\omega, \boldsymbol{k})$. (S9)

Substituting Eq. S7, into Eq. S9 we find

$\langle \delta c^*(t)^2 \rangle = \frac{A\beta^2 \bar{c}^2 (D_2 k^2)^2}{2(D_2 k^2 + k_{endo})}$.(S10)

Replacing Eq. S8 into Eq. S10 we obtain

$A = \frac{2(D_2 k^2 + k_{endo})}{\bar{c}\beta^2\, (D_2 k^2)^2}$, (S11)

and hence the power spectrum $S_c(\omega, \boldsymbol{k})$ becomes

$S_c(\omega, \boldsymbol{k}) = \frac{2\bar{c}(D_2 k^2 + k_{endo})}{\omega^2 + (D_2 k^2 + k_{endo})^2}$. (S12)

This expression is a generalization of the correlation function of the fluctuations of the number of solute particles in a weak solution where particles are continuously recycled (6). Next, we consider a receptor that can measure ligand concentration in a radius roughly equivalent to its size, a, over an integration time τ. The average ligand concentration measured by a receptor will be given by

$$\tilde{c}(t,x) = \int d^2x'dt'\, w_r(\boldsymbol{x}-\boldsymbol{x}')k_r(t-t')\, c(t',\boldsymbol{x}'). \text{ (S13)}$$

where the function $w_r(\boldsymbol{x}-\boldsymbol{x}')$ defines the receptor spatial distribution and $k_r(t-t')$ describes the receptor temporal response. We take the limit of a 'perfect' receptor which can count all the ligands that arrive at its close vicinity.

We choose Gaussian distributions $w_r(\boldsymbol{x}-\boldsymbol{x}') = \frac{e^{-(x-x')^2/(2a^2)}}{2\pi a^2}$ and

$k_r(t-t') = \frac{e^{-(t-t')^2/(2\tau^2)}}{\sqrt{2\pi}\tau}$.

Both Gaussian distributions are normalized: $\int d^2\, x\, w_r(\boldsymbol{x}-\boldsymbol{x}') = 1$ and $\int dt\ k_r(t-t') = 1$. As a matter of comparison, note that a slightly different kernel function $w_j(t)$ was defined by Berg and Purcell (7), being equal to 1 if the ligand molecule is at time t inside a small sphere representing a receptor and 0 otherwise.

Using Eq. S13, and writing $\delta c^*(t',\boldsymbol{x}')$ in terms of its Fourier transform, we find that $\langle\delta\tilde{c}(t,\boldsymbol{x})^2\rangle$ is given by

$$\langle\delta\tilde{c}(t,\boldsymbol{x})\delta\tilde{c}(t,\boldsymbol{x})\rangle = \int d^2x'dt'd\omega\,\frac{d^2k}{(2\pi)^3}\,d^2x''dt''\,d\omega'\,\frac{d^2k'}{(2\pi)^3}$$

$$w_r\left(\boldsymbol{x}-\boldsymbol{x}'\right)k_r\left(t-t'\right)e^{i\left(\boldsymbol{k}\cdot\boldsymbol{x}'-\omega t'\right)}w_r\left(\boldsymbol{x}-\boldsymbol{x}''\right)k_r\left(t-t''\right)e^{i\left(\boldsymbol{k}'\cdot\boldsymbol{x}''-\omega' t''\right)}\langle\delta c^*(\omega,\boldsymbol{k})\delta c^*\left(\omega',\boldsymbol{k}'\right)\rangle$$

$$= \int d^2x'dt'd\omega\,\frac{d^2k}{(2\pi)^3}\,\mathrm{d}^2x''dt''$$

$$d\omega'\,\frac{d^2k'}{(2\pi)^3}\,\frac{e^{-(t-t')^2/(2\tau^2)}}{\sqrt{2\pi}\tau}\,\frac{e^{-(x-x')^2/(2a^2)}}{2\pi a^2}\,e^{i(\boldsymbol{k}\cdot\boldsymbol{x}'-\omega t')}\,\frac{e^{-(t-t'')^2/(2\tau^2)}}{\sqrt{2\pi}\tau}\,\frac{e^{-(x-x'')^2/(2a^2)}}{2\pi a^2}\,e^{i(\boldsymbol{k}'\cdot\boldsymbol{x}''-\omega' t'')}$$

$\langle\delta c^*(\omega,\boldsymbol{k})\delta c^*(\omega',\boldsymbol{k}')\rangle$. (S14)

It is easy to see that

$$\int dt'\,\frac{e^{-(t-t')^2/(2\tau^2)}}{\sqrt{2\pi}\tau}\,e^{-i\omega t'} = e^{-i\omega t}e^{-\tau^2\omega^2/2}\text{ , (S15)}$$

and

$$\int d^2x'\,\frac{e^{-(x-x')^2/(2a^2)}}{2\pi a^2}\,e^{i\boldsymbol{k}\cdot\boldsymbol{x}'} = e^{i\boldsymbol{k}\cdot\boldsymbol{x}}e^{-a^2k^2/2}\text{. (S16)}$$

Then taking into account that $(\langle \delta c^*(\omega, \boldsymbol{k}) \delta c^*(\omega', \boldsymbol{k}') \rangle = (2\pi)^3 \delta(\omega + \omega') \delta(\boldsymbol{k} + \boldsymbol{k}') S_{c^*}(\omega, \boldsymbol{k}))$ (4), we obtain

$$\langle \delta \tilde{c}^2 \rangle = \int \frac{d\omega d^2k}{(2\pi)^3} \frac{2\bar{c}(D_2 k^2 + k_{endo})}{\omega^2 + (D_2 k^2 + k_{endo})^2} e^{-\tau^2 \omega^2} e^{-a^2 k^2} \quad \text{(S17)}$$

where $\langle \delta \tilde{c}^2 \rangle = \langle \delta \tilde{c}(t, \boldsymbol{x}) \delta \tilde{c}(t, \boldsymbol{x}) \rangle$.

Due to the radial symmetry of the function appearing in Eq. S17 it is natural to introduce polar coordinates $(k = |\boldsymbol{k}|, \theta)$. After performing the integration in the azimuthal angle, Eq. S17 can be rewritten as

$$\langle \delta \tilde{c}^2 \rangle = \int_{-\infty}^{\infty} d\omega \, e^{-\tau^2 \omega^2} \int_0^{\infty} \frac{kdk}{(2\pi)^2} e^{-a^2 k^2} \frac{2\bar{c}(D_2 k^2 + k_{endo})}{\omega^2 + (D_2 k^2 + k_{endo})^2}. \text{(S18)}$$

In order to compute Eq. S18 we introduce the following dimensionless parameters

$$\alpha = \frac{a^2}{D_2 \tau}, \; v = ka, u = \omega\tau.$$

Then $\langle \delta \tilde{c}(t, x)^2 \rangle$ becomes

$$\langle \delta \tilde{c}^2 \rangle = \frac{\bar{c}\alpha}{\pi^2 a^2} \int_0^{\infty} du \, e^{-u^2} \int_0^{\infty} dv \, e^{-v^2} \frac{v(v^2 + \alpha k_{endo} \tau)}{\alpha^2 u^2 + (v^2 + \alpha k_{endo} \tau)^2} =$$

$$\frac{\bar{c}\alpha}{\pi^2 a^2} \int_0^{\infty} du \, e^{-u^2} \int_0^{\infty} dv \, e^{-v^2} \frac{v\left(v^2 + \left(\frac{a}{\lambda}\right)^2\right)}{\alpha^2 u^2 + (v^2 + \left(\frac{a}{\lambda}\right)^2)^2}, \text{(S19)}$$

where we define the diffusive length scale $\lambda = \sqrt{\frac{D_2}{k_{endo}}}$.

The parameter *a* for typical receptors is about 1-10 *nm*, D_2 is in the range 0.01-0.1 μm^2/sec (8,9), and k_{endo} varies in the range 0.001-0.01 1/sec (10-13).

Hence we have $\left(\frac{a}{\lambda}\right)^2 \sim 10^{-8} - 10^{-5} \ll 1$. The parameter α^2 for large integration times is expected to be in the range $[10^{-16}, 10^{-10}]$.

The u –integrand, due to the term e^{-u^2}, tends to zero for $u \sim 2$. Then, introducing a sharp cut-off $u_{max} = \pi$, or $(\omega_{max} = \frac{\pi}{\tau})$, we may approximate the integral from 0 to ∞ of the Gaussian by an integral with a sharp cutoff and the Gaussian substituted by 1. Hence we proceed by evaluating the *u* integral,

$$\langle \delta \tilde{c}^2 \rangle = \frac{\bar{c}\alpha}{\pi^2 a^2} \int_0^{\pi} du \int_0^{\infty} dv \, e^{-v^2} \frac{v\left(v^2 + \left(\frac{a}{\lambda}\right)^2\right)}{\alpha^2 u^2 + (v^2 + \left(\frac{a}{\lambda}\right)^2)^2} = \frac{\bar{c}\alpha}{\pi^2 a^2} \int_0^{\infty} dv \, e^{-v^2} v \left(v^2 + \left(\frac{a}{\lambda}\right)^2\right) \frac{\arctan\left(\frac{\alpha\pi}{v^2 + \left(\frac{a}{\lambda}\right)^2}\right)}{\alpha(v^2 + \left(\frac{a}{\lambda}\right)^2)} = \frac{\bar{c}}{\pi^2 a^2} \int_0^{\infty} dv \, e^{-v^2} v \arctan\left(\frac{\alpha\pi}{v^2 + \left(\frac{a}{\lambda}\right)^2}\right). \text{(S20)}$$

The v −integrand of Eq. S20, drops to almost 0 for $v\sim 2$, due to the exponential function e^{-v^2} and that the function $\frac{v\left(v^2+\left(\frac{a}{\lambda}\right)^2\right)}{\alpha^2u^2+(v^2+\left(\frac{a}{\lambda}\right)^2)^2}$ is bounded. Therefore most of the contribution to the integral (Eq. S20) comes from values of $v<2$. We simplify the calculation by approximating the v-integral appearing in Eq. S20 by a new integral with a sharp cut-off $v_{max}=1$ (i.e. $k_{max}=\frac{1}{a}$) where the function e^{-v^2} is replaced by 1 (2,14) (see below, Eq. S21).

Defining $\delta c=\sqrt{\langle\delta\tilde{c}^2\rangle}$, and recalling that the argument of the $arctan$ is small for large enough integration times ($\alpha\ll\left(\frac{a}{\lambda}\right)^2$, or equivalently $\tau\gg\frac{1}{k_{endo}}$), we finally obtain

$$\left(\frac{\delta c}{\bar{c}}\right)^2=\frac{\alpha}{\pi^2a^2}\int_0^1 dv\ \frac{\pi v}{v^2+\left(\frac{a}{\lambda}\right)^2}=\frac{1}{\pi D_2\tau\bar{c}}\ln\left(\frac{\lambda}{a}\right),\ \text{(S21)}$$

where we have assumed that $\frac{\lambda}{a}\gg 1$.

For the case of short integration times ($\tau\ll\frac{1}{k_{endo}}$) we proceed by first evaluating the v −integral (here we also assumed a sharp cutoff to take care of the integrands containing the Gaussians)

$$\langle\delta\tilde{c}^2\rangle=\frac{\bar{c}\alpha}{\pi^2a^2}\int_0^\pi du\int_0^1 dv\ \frac{v\left(v^2+\left(\frac{a}{\lambda}\right)^2\right)}{\alpha^2u^2+(v^2+\left(\frac{a}{\lambda}\right)^2)^2}.\ \text{(S22)}$$

The v integral can be evaluated analytically using the expression $\int dv\frac{v(v^2+l)}{b^2+(v^2+a)^2}=\frac{1}{4}\ln[b^2+(v^2+l)^2]$. Hence Eq.S22 is equivalent to

$$\langle\delta\tilde{c}^2\rangle=\frac{\bar{c}\alpha}{\pi^2a^2}\int_0^\pi du\frac{1}{4}\ln(1+\frac{(2\left(\frac{a}{\lambda}\right)^2+1)}{\left(\frac{a}{\lambda}\right)^4+\alpha^2u^2}).\ \text{(S23)}$$

This integral can be computed analytically using

$$\int dx ln(1+\frac{a}{b+cx^2})=xln\left(\frac{a}{b+cx^2}+1\right)+\frac{2\sqrt{a+b}\,tan^{-1}(\frac{\sqrt{c}\,x}{\sqrt{a+b}})}{\sqrt{c}}-2\sqrt{\frac{b}{c}}tan^{-1}(\sqrt{\frac{c}{b}}x),\quad\text{then}$$

we obtain

$$\langle \delta\tilde{c}^2 \rangle =$$

$$\frac{\bar{c}\alpha}{\pi^2 a^2}\frac{1}{4}\left[\ln\left(1+\frac{\left(2\left(\frac{a}{\lambda}\right)^2+1\right)}{\left(\frac{a}{\lambda}\right)^4+\alpha^2}\right)+\frac{2}{\alpha}\sqrt{\left(2\left(\frac{a}{\lambda}\right)^2+1\right)+\left(\frac{a}{\lambda}\right)^4}\,tan^{-1}\left(\frac{\alpha}{\sqrt{\left(2\left(\frac{a}{\lambda}\right)^2+1\right)+\left(\frac{a}{\lambda}\right)^4}}\right)-\right.$$

$$\left.\frac{2k_{endo}\tau}{\alpha}\,tan^{-1}\left(\frac{\alpha}{k_{endo}\tau}\right)\right]. \text{ (S24)}$$

Note that the expression shown in Eq.S24 is valid for any integration time τ.

In the limit $\left(\frac{a}{\lambda}\right)^2 \ll 1$, and assuming $\left(\frac{a}{\lambda}\right)^4 \ll \alpha^2$ (i.e. $\tau \ll \frac{1}{k_{endo}}$, for short integration times), we find that

$$\langle \delta\tilde{c}^2 \rangle = \frac{\bar{c}\alpha}{\pi a^2}\frac{1}{4}\left[\ln\left(1+\frac{1}{\alpha^2}\right)+\frac{2}{\alpha}tan^{-1}\alpha-\frac{2k_{endo}\tau}{\alpha}\,tan^{-1}\left(\frac{\alpha}{k_{endo}\tau}\right)\right]. \text{ (S25)}$$

The parameter α is expected to be in the range $(10^{-4}-10^{-1})$. The term $\ln\left(\frac{1}{\alpha^2}+1\right)$ may be approximated by $\ln\left(\frac{1}{\alpha^2}\right)$. The difference between the terms $\frac{2}{\alpha}tan^{-1}\alpha$, and $\frac{2k_{endo}\tau}{\alpha}\,tan^{-1}\left(\frac{\alpha}{k_{endo}\tau}\right)$, is small compared to the $\ln\left(\frac{1}{\alpha^2}\right)$ term . Hence we get that, for short integration times,

$\langle \delta\tilde{c}^2 \rangle = \frac{\bar{c}}{\pi D_2 \tau}\ln\left(\sqrt{\frac{D_2\tau}{a^2}}\right) = \frac{\bar{c}}{\pi D_2 \tau}\ln\left(\frac{\lambda^*}{a}\right)$, where $\lambda^* \equiv \sqrt{D_2\tau}$ is the corresponding natural length scale. Then the relative uncertainty for short integration times becomes

$$\left(\frac{\delta c}{\bar{c}}\right)^2 = \frac{1}{\pi D_2 \tau \bar{c}}\ln\left(\frac{\lambda^*}{a}\right). \text{ (S26)}$$

By plotting the function defined by Eq.S24 it is easy to verify that the limits given by Eqs. S21 and S26 are good approximations for the accuracy at short and large integration times.

Note that in the very extreme case where α gets so large (i.e. integration time very close to 0, or very small diffusion coefficient) that the dominant term in Eq. S24 is the second term, $\frac{2}{\alpha}tan^{-1}(\alpha)\sim\frac{\pi}{\alpha}$, then we get $\langle \delta\tilde{c}^2 \rangle = \frac{\bar{c}\alpha}{\pi^2 a^2}\frac{1}{4}\frac{\pi}{\alpha}$ and $\left(\frac{\delta c}{\bar{c}}\right)^2 = \frac{1}{4\pi\bar{c}a^2}$. Time average does not appear, but just the size of the receptor. In this limit the ligands can hardy diffuse over distances larger than the receptor size, and then it makes sense that there will not be any diffusion noise. Without diffusion the only

source of noise would be Poisson counting noise $\frac{1}{\sqrt{N}}$, where N is the number of ligands placed in the contact area (namely, $\left(\frac{\delta c}{\bar{c}}\right)^2 \sim \frac{1}{a^2\bar{c}}$).

Accuracy of ligand concentration measurement by multiple receptors

In order to take into account the presence of *m* multiple receptors, we assume

$\delta\tilde{c}(t,\boldsymbol{x}) = \sum_{\mu=1}^{m} \int d^2x dt'\, w_r(\boldsymbol{x_\mu} - \boldsymbol{x'}) k_r(t-t')\, \delta c^*(t', \boldsymbol{x'})$, (S27)

where $w_r(\boldsymbol{x_\mu} - \boldsymbol{x'}) = \frac{e^{-(x_\mu - x\prime)^2/(2a^2)}}{2\pi a^2 m}$. (S28)

Proceeding in a similar way to the case of one receptor, we compute $\langle\delta\tilde{c}^2\rangle$:

$\langle\delta\tilde{c}^2\rangle = \sum_{\mu,\nu} \int d^2x' dt' d\omega \frac{d^2k}{(2\pi)^3} d^2x'' \mathrm{d}t''$

$d\omega' \frac{d^2k'}{(2\pi)^3} \frac{e^{-(x_\mu - x\prime)^2/(2a^2)}}{2\pi a^2 m} \frac{e^{-(t-t')^2/(2\tau^2)}}{\sqrt{2\pi}\tau} \frac{e^{-(x'' - x_\nu)^2/(2a^2)}}{2\pi a^2 m} \frac{e^{-(t-t'')^2/(2\tau^2)}}{\sqrt{2\pi}\tau} e^{i(\boldsymbol{k}\cdot\boldsymbol{x'} - \omega t')}$

$e^{i(\boldsymbol{k'}\cdot\boldsymbol{x''} - \omega' t')} \langle \delta c^*(\omega, \boldsymbol{k}) \delta c^*(\omega', \boldsymbol{k'}) \rangle$. (S29)

As in the one receptor case, we set $\omega' = -\omega$ and $\boldsymbol{k'} = -\boldsymbol{k}$ (4), and obtain

$\langle\delta\tilde{c}^2\rangle = \sum_{\mu,\nu} \int d\omega \frac{d^2k}{(2\pi)^3}\, e^{-\tau^2\omega^2} e^{-a^2k^2} (\frac{1}{m})^2 e^{i\boldsymbol{k}\cdot\boldsymbol{x_\mu}} e^{-i\boldsymbol{k}\cdot\boldsymbol{x_\nu}} \frac{2\bar{c}(D_2k^2 + k_{endo})}{\omega^2 + (D_2k^2 + k_{endo})^2}$. (S30)

We first consider low frequencies ($\omega \approx 0$) (2). Then we replace the infinite integral in ω (Eq.S30) by an integral with sharp cutoff $\omega_{max} \sim \frac{\pi}{\tau}$ and substitute the Gaussian kernel by the constant value 1 (similarly to the case of one receptor). Then Eq.S30 can be rewritten as

$\langle\delta\tilde{c}^2\rangle = \sum_{\mu,\nu} \int_0^\infty d\omega \int \frac{d^2k}{(2\pi)^3} e^{-\tau^2\omega^2} e^{-a^2k^2} e^{i\boldsymbol{k}\cdot(\boldsymbol{x_\mu} - \boldsymbol{x_\nu})} (\frac{1}{m})^2 \frac{4\bar{c}(D_2k^2 + k_{endo})}{\omega^2 + (D_2k^2 + k_{endo})^2}$ (S31).

The integral in ω is just $\frac{\pi}{\tau}$, therefore Eq.S31 becomes

$\langle\delta\tilde{c}^2\rangle \sim \sum_{\mu,\nu} \int \frac{d^2k}{(2\pi)^3}\, e^{-a^2k^2} e^{i\boldsymbol{k}\cdot(\boldsymbol{x_\mu} - \boldsymbol{x_\nu})} (\frac{1}{m})^2 \frac{4\pi\bar{c}/(D_2\tau)}{k^2 + k_{endo}/D_2}$ (S32).

The dominant terms in Eq.S32 come from the terms with small ka, due to the drop of the Gaussian kernel. Therefore, we may approximate the Gaussian by the constant 1 and limit the integral in k from 0 to $\frac{1}{a}$. Note that the integral (in Eq. S32) is in addition highly oscillatory for large values of k. In particular, the Fourier integral is highly oscillatory in the exponent $\boldsymbol{k}\cdot(\boldsymbol{x_\mu} - \boldsymbol{x_\nu})$. The maximal value of k contributing to the integral is $k_{max} \sim \frac{1}{|\boldsymbol{x_\mu} - \boldsymbol{x_\nu}|_{min}} \sim 1/a$. Therefore we may consider

the integral again over all possible values of k, because large values of k do not contribute to the Fourier integral. Hence Eq. S32 is replaced by

$$\langle \delta\tilde{c}^2 \rangle \approx \sum_{\mu,\nu} \left(\frac{1}{m^2}\right) \frac{4\pi\bar{c}}{D_2\tau} \int \frac{d^2k}{(2\pi)^3} e^{i\boldsymbol{k}\cdot(\boldsymbol{x_\mu}-\boldsymbol{x_\nu})} \frac{1}{k^2+\left(\frac{1}{\lambda}\right)^2}. \quad \text{(S33)}$$

Now the integral term appearing in Eq. S33 is the 2D inverse Fourier transform of the generalized function $\frac{1}{k^2+\left(\frac{1}{\lambda}\right)^2}$. This corresponds to one of the well-known radial inverse Fourier transform, and it can be written in terms of the modified Bessel function K_0 (15-18).

$$\int d^2k \, \frac{e^{i\boldsymbol{k}\cdot\boldsymbol{r}}}{k^2+\frac{1}{\Lambda^2}} = 2\pi K_0\left(\frac{|\boldsymbol{r}|}{\Lambda}\right). \quad \text{(S34)}$$

Therefore, Eq. S33 can be expressed as

$$\langle \delta\tilde{c}^2 \rangle \approx \sum_{\mu\neq\nu} \left(\frac{1}{m^2}\right) \frac{\bar{c}}{\tau D_2 \pi} K_0\left(|\boldsymbol{x_\mu} - \boldsymbol{x_\nu}|/\lambda\right) + \frac{\bar{c}}{\pi m \tau D_2} \ln\left(\frac{\lambda}{a}\right). \quad \text{(S35)}$$

The only limitations of Eq.S35 are $\frac{\lambda}{a} \gg 1$ and $\tau \gg \frac{1}{k_{endo}}$.

For the sake of simplicity, we will assume a cluster of m receptors of size *a* distributed equidistantly along a ring of radius *s* (2). This assumption allows us to simplify Eq. S35.

Let's define the following variables

$$\theta_i = i\frac{2\pi}{m}, \; x_1 = 0, y_1 = s, x_i = s\, sin\theta_i, y_i = s\, cos\theta_i. \quad \text{(S36)}$$

It is easy to see that

$$|(x_1 - x_i)| = \sqrt{2}s\sqrt{1 - cos\theta_i} = 2s\, \sin(\frac{\pi i}{m}). \quad \text{(S37)}$$

Therefore, defining $\delta c = \sqrt{\langle \delta\tilde{c}^2 \rangle}$ we obtain for large integration times

$$\left(\frac{\delta c}{\bar{c}}\right)^2 \approx \left[\frac{\ln(\frac{\lambda}{a})}{\pi m D_2 \bar{c}\tau} + \frac{\sum_{i=1}^{m-1} K_0(\frac{2s}{\lambda_1}\sin(\frac{\pi i}{m}))}{\pi m D_2 \bar{c}\tau}\right], \quad \text{(S38)}$$

or

$$\left(\frac{\delta c}{\bar{c}}\right) \approx \frac{1}{\sqrt{\pi D_2 \bar{c}\tau m}} \sqrt{\ln\left(\frac{\lambda}{a}\right) + \sum_{i=1}^{m-1} K_0\left(\frac{2s}{\lambda}\sin\left(\frac{\pi i}{m}\right)\right)}. \quad \text{(S39)}$$

As a limiting case we consider $\lambda \gg s$. In this case we can use the limiting form for the modified Bessel function K_0 for $x \ll 1$ (18):

$$K_0(x \ll 1) \approx -\left(\ln\left(\frac{x}{2}\right) + C\right), \qquad \text{(S40)}$$

where C=0.5772 (Euler-Mascheroni constant).

Using the identity (18):

$$\sin(\pi m\varphi) = 2^{m-1}\prod_{i=0}^{m-1} sin\pi(\frac{i}{m} + \varphi), \text{ (S41)}$$

it is easy to show that

$$\prod_{i=1}^{m-1} sin\left(\frac{\pi i}{m}\right) = 2^{1-m}m, \text{ for m≥2 . (S42)}$$

Therefore, the sum of modified Bessel functions can be approximated as follows

$$\sum_{i=1}^{m-1} K_0\left(\frac{2s}{\lambda}\sin\left(\frac{\pi i}{m}\right)\right) = -\sum_{i=1}^{m-1} ln\left(\frac{s}{\lambda}\sin\left(\frac{\pi i}{m}\right)\right) + C = -\sum_{i=1}^{m-1} ln\left(\frac{se^C}{\lambda}\sin\left(\frac{\pi i}{m}\right)\right) =$$

$$\prod_{i=1}^{m-1} ln\left(\frac{se^C}{\lambda}\sin\left(\frac{\pi i}{m}\right)\right) = -\ln[\left(\frac{se^C}{\lambda}\right)^{m-1} 2^{1-m}m] = -\Bigg((m-1)\ln\left(\frac{se^C}{2\lambda}\right) + \ln(m)\Bigg) = (m-1)\ln\left(\frac{2\lambda}{se^C}\right) - \ln(m). \qquad \text{(S43)}$$

Substituting Eq. S43 into Eq. S39 we obtain the final result

$$\frac{\delta c}{\bar{c}} \approx \frac{1}{\sqrt{\pi D_2 \bar{c}\tau}}\sqrt{\frac{\ln\left(\frac{\lambda}{ma}\right)}{m} + \left(\frac{m-1}{m}\right)\ln\left(1.1228\frac{\lambda}{s}\right)}. \qquad \text{(S44)}$$

It should be mentioned that this same result was obtained by introducing internal noise to the receptor-ligand system and computing the accuracy using the fluctuation dissipation theorem (see below).

Calculation of accuracy in the absence of endocytosis

We start with Eq.S30 and consider the limit case $k_{endo} = 0$. Then

$$\left\langle\left(\frac{\delta c}{\bar{c}}\right)^2\right\rangle = \sum_{\mu,\nu}\int_0^\infty d\omega\,\frac{d^2k}{(2\pi)^3}\, e^{-\tau^2\omega^2}e^{-a^2k^2}\left(\frac{1}{m}\right)^2 e^{i\boldsymbol{k}\cdot\boldsymbol{x_\mu}}e^{-i\boldsymbol{k}\cdot\boldsymbol{x_\nu}}\frac{4D_2k^2}{\omega^2+(D_2k^2)^2}. \text{ (S45)}$$

In order to perform the ω-integral we assume a cutoff at $\omega_{max}\sim\frac{\pi}{\tau}$, and approximate the Gaussian by the constant 1 in the low frequency limit $\omega \approx 0$ (similarly to the way we computed Eq.S30). Then the integral in ω is just $\frac{\pi}{\tau}$ and we obtain

$$\left\langle\left(\frac{\delta c}{\bar{c}}\right)^2\right\rangle = \frac{4\pi}{\bar{c}\tau}\sum_{\mu,\nu}\int\frac{d^2k}{(2\pi)^3}\, e^{-a^2k^2}\left(\frac{1}{m}\right)^2 e^{i\boldsymbol{k}\cdot\boldsymbol{x_\mu}}e^{-i\boldsymbol{k}\cdot\boldsymbol{x_\nu}}\,\frac{1}{D_2k^2}. \text{ (S46)}$$

In order to compute the integral in Eq.S46 we will follow also an approach similar to the one we used to compute Eq. S32. We note that the major contributions come from small values of , again this is due to the Gaussian kernel $e^{-a^2k^2}$ that drops for $k \gg \frac{1}{a}$ and also because the Fourier integral is highly oscillatory in the exponent $\boldsymbol{k}\cdot(\boldsymbol{x_\mu}-\boldsymbol{x_\nu})$. We can see that the maximal value of k contributing to the integral is $k_{max}\sim\frac{1}{|\boldsymbol{x_\mu}-\boldsymbol{x_\nu}|_{min}}\sim 1/a$. Therefore the procedure is to approximate the Gaussian by 1, and then compute Eq.S46 using Fourier transform of radial functions (15). Hence we obtain

$$\left(\frac{\delta c}{\bar{c}}\right)^2 \approx \sum_{\mu,\nu}\left(\frac{1}{m^2}\right)\frac{4\pi}{D_2\tau\bar{c}}\int\frac{d^2k}{(2\pi)^3}\, e^{i\boldsymbol{k}\cdot(\boldsymbol{x_\mu}-\boldsymbol{x_\nu})}\frac{1}{k^2} = -\sum_{\mu\neq\nu}\frac{1}{\pi m D_2\tau\bar{c}}\left(\ln\left[\frac{|\boldsymbol{x_\mu}-\boldsymbol{x_\nu}|}{\lambda^*}\right]+C\right)+ \frac{1}{m\pi D_2\tau\bar{c}}\ln\left(\frac{\sqrt{D_2\tau}}{a}\right). \text{(S47)}$$

where C~0.5772, and λ^* is a typical length scale. We adopt $\lambda^* \sim\sqrt{D_2\tau}$. The length scale λ^* (in the absence of endocytosis) plays the role of the length scale $\lambda = \sqrt{\frac{D_2}{k_{endo}}}$ present when endocytosis is involved. An additional justification for the typical length scale $\lambda^* \equiv \sqrt{D_2\tau}$ in the absence of endocytosis is shown using the FDT (see below section dedicated to the FDT approach).

Hence the accuracy will be given by

$$\left(\frac{\delta c}{\bar{c}}\right)^2 = \frac{1}{m\pi D_2\tau\bar{c}}\ln\left(\frac{\sqrt{D_2\tau}}{a}\right) - \frac{1}{\pi m D_2\tau\bar{c}}\left(\sum_{i=1}^{m-1} ln\left(\frac{s}{\sqrt{D_2\tau}}\sin\left(\frac{\pi i}{m}\right)\right)+C\right). \text{(S48)}$$

The second term involving $\sum_{i=1}^{m-1} ln\left(\frac{s}{\sqrt{D_2\tau}}\sin\left(\frac{\pi i}{m}\right)\right)$ can be simplified. Then we may use the result of Eq.S43 and obtain

$$\left(\frac{\delta c}{\bar{c}}\right)^2 = \frac{1}{\pi D_2\tau\bar{c}}\left[\frac{\ln\left(\frac{\sqrt{D_2\tau}}{ma}\right)}{m}+\left(\frac{m-1}{m}\right)\ln\left(1.1228\frac{\sqrt{D_2\tau}}{s}\right)\right] \text{(S49)}$$

For large number of receptors we may just use the approximate expression $\left(\frac{\delta c}{\bar{c}}\right)^2 = \frac{1}{\pi D_2\tau\bar{c}}\ln\left(1.1228\frac{\sqrt{D_2\tau}}{s}\right)$. (S50).

Note that this expression has a physical meaning only for $\lambda^* > s$.

Note that in the absent of endocytosis and assuming $\frac{s}{\sqrt{D_2\tau}} \ll 1$, we obtained an expression for the accuracy (Eq.S49) similar to the one obtained when endocytosis is present and $\lambda \gg s$ (Eq.S44). We infer that for more general cases, i.e. where the contact radio is larger than the typical length scale $\lambda^* \equiv \sqrt{D_2\tau}$, the accuracy for short integration times will be given by the expression Eq. S39 but with λ replaced by λ^*.

One way of seeing this is by noticing that for short integration times, endocytosis role is negligible, being λ^* the only relevant length scale affecting the accuracy.

Improvement of accuracy by averaging over neighboring cells

We assume that each cell is surrounded by *N* neighboring cells and receives a signal from all its neighbors. The total signal received by the cell, *S(t)*, is the sum of the individual signals from all its neighbors. Assuming that the signal from each neighbor is proportional to its ligand concentration we can write

$$S(t) = \sum_{i=1}^{N} c_i\,(t) \quad \text{(S51)}$$

(for simplicity we assumed that the proportionality constant is 1). The average value of the signal measured by all neighbor cells is given by $\bar{S_1}(t) = \sum_{i=1}^{N} \bar{c}_i\,(t)$.

The accuracy of the total signal is therefore defined as

$$\delta S = S - \bar{S} = \sum_{i=1}^{N}(c_i\text{-}\bar{c}_i)=\sum_{i=1}^{N} \delta c_i. \quad \text{(S52)}$$

Squaring both terms we obtain

$$(\delta S)^2 = \sum_{i=1}^{N}(\delta c_i)^2 + \sum_{i,i\neq j}\sum_{j}(\delta c_i)\left(\delta c_j\right). \quad \text{(S53)}$$

We take ensemble average of Eq. S53. Assuming that the measurements performed by each neighbor cell are statistically independent, and since $\langle(\delta c_i)\rangle = 0$, we see that $\langle(\delta c_i)\left(\delta c_j\right)\rangle = \langle(\delta c_i)\rangle\,\langle\left(\delta c_j\right)\rangle = 0$, and hence $\langle(\delta S)^2\rangle = \sum_{i=1}^{N}\langle(\delta c_i)^2\rangle$. (S54)

The relative accuracy of measuring ligand concentration $\frac{\langle(\delta S_1)^2\rangle}{\bar{S_1}^2}$ turns out to be

$$\frac{\langle(\delta S)^2\rangle}{\bar{S}^2} = \frac{\sum_{i=1}^{N}\langle(\delta c_i)^2\rangle}{(\sum_{i=1}^{N}\bar{c}_i)^2} \quad \text{(S55)}$$

There are several interesting limiting cases.

First case: If ligand concentration in all neighbors is approximately the same, namely $c_i \approx c_0$, where c_0 is the average concentration in a tissue. We then get

$$\frac{(\delta S)^2}{\bar{S}^2} = \frac{(\delta c_0)^2}{N c_0^2}\,. \quad \text{(S56)}$$

We note that averaging by *N* neighbor cells the accuracy gets improved by a factor of $\frac{1}{\sqrt{N}}$, as expected from averaging N independent random variables.

Second case: The ligand concentration in one of the cells is much larger than in the other cells, $c_i \gg c_{j\neq i}$. Then, defining $c_i = c_0$,

$$\frac{(\delta S)^2}{\bar{S}^2} = \frac{(\delta c_0)^2}{c_0^2}\,. \qquad \text{(S57)}$$

In this case the noise is dominated by the cell with the higher ligand concentration.

Third case: There is a gradient of ligand concentration (as in the vein boundary case discussed in the text). Assuming a two dimensional array of hexagonal cells (*N*=6 neighbors) and a linear gradient in ligand concentration we can write the concentration in each of the cells as:

$$c_{i-1,j-1} = c_0(1+\frac{a}{2});\ c_{i+1,j-1} = c_0(1-\frac{a}{2});\ \ c_{i-1,j} = c_0(1+a);\ c_{i+1,j} = c_0(1-a);$$
$$c_{i-1,j+1} = c_0(1+\frac{a}{2});\ c_{i+1,j+1} = c_0\left(1-\frac{a}{2}\right). \qquad \text{(S58)}$$

where $c_{i,j}$ denotes the ligand concentration measured by the cell located at row *i* and column *j*.

In this case, since $\sum(\delta c_{i,j})^2$=6$(\delta c_0)^2$ we get the same result as with a uniform ligand concentration with $c_i = c_0$.

Processing of receptor-ligand pair improves accuracy by a factor of up to $\sqrt{2}$

We consider a receptor with radius *a.* Every ligand molecule reaching the receptor is immediately absorbed, hence we may assume that the ligand concentration is zero at the border of the receptor *r=a*. We also assume that there is a constant ligand concentration far away. The ligand concentration satisfies the diffusion equation

$$\frac{\partial c(\boldsymbol{x},t)}{\partial t} = D_2\nabla^2 c - k_{endo}c(x,t) + k_{exo}c_{cyto} \quad \text{(S59)}$$

with the boundary condition $c(r=a)=0$, meaning the ligand molecules are trapped as soon as they reach the receptor. The second condition corresponds to a reflective boundary $\frac{\partial c}{\partial r}(r=b)=0$. This means that same number of ligands is crossing back and forth the external boundary $r=b$ (20).
Due to the symmetry of the problem, we introduce polar coordinates. Then the steady state solution will satisfy the following ODE:
$D_2\frac{1}{r}\frac{d}{dr}\left(r\frac{dc}{dr}\right) - k_{endo}c(r,t) + \beta = 0$ (S60),
where $\beta = k_{exo}c_{cyto}$.
In order to solve this equation, we define $c = c^* + \frac{\beta}{k_{endo}}$. Therefore c^* satisfies the equation
$\frac{1}{r}\left[D\frac{\partial c^*}{\partial r} + Dr\frac{\partial^2 c^*}{\partial r^2}\right] - r^2 k_{endo}c^* = 0$(S61).
This corresponds to a Modified Bessel's equation.
The most general solution of this equation can be written in terms of the modified Bessel functions as
$c^*(r) = AI_0\left(\frac{r}{\lambda}\right) + BK_0\left(\frac{r}{\lambda}\right)$ (S62),

where $= \sqrt{\frac{D_2}{k_{endo}}}$, and I_0, K_0 are the modified Bessel functions of order 0 (18).
Then it is very easy to show that the solution to this boundary value problem (perfect absorbing receptor) is
$c(r) = \frac{\beta}{k_{endo}}\left[1 - \frac{I_1\left(\frac{b}{\lambda}\right)K_0\left(\frac{r}{\lambda}\right)+K_1\left(\frac{b}{\lambda}\right)I_0\left(\frac{r}{\lambda}\right)}{I_1\left(\frac{b}{\lambda}\right)K_0\left(\frac{a}{\lambda}\right)+K_1\left(\frac{b}{\lambda}\right)I_0\left(\frac{a}{\lambda}\right)}\right]$ (S63),
I_0, K_0 and K_1 are the modified Bessel functions of order 0 and 1 (18).

In order to find the flux at the receptor's border we need to compute the current $J_r = D_2\frac{\partial c}{\partial r}$. The number of ligand molecules impinging on the receptor per unit time is given by $J_r 2\pi a$. Then, the rate of particles absorbed by the receptor during an integration time τ is given by $N = J_r 2\pi a\tau$.
The ligands behave independently; therefore we assume they are distributed according to Poisson distribution, $\langle(\delta N)^2\rangle = \langle N\rangle$. Hence, for a perfectly absorbing receptor the uncertainty in measuring ligands concentration is given by (21)
$\left(\frac{\delta c}{\bar{c}}\right)^2 = \frac{\langle(\delta N)^2\rangle}{\langle N\rangle^2} = \frac{1}{\langle N\rangle} = \frac{1}{J_r 2\pi a\tau}$ (S64).
Let's compute the flux:

$J_r = D_2\frac{\partial c}{\partial r} = -\frac{D_2\beta}{k_{endo}}\left[\frac{I_1\left(\frac{b}{\lambda}\right)\frac{d}{dr}K_0\left(\frac{r}{\lambda}\right)+K_1\left(\frac{b}{\lambda}\right)\frac{d}{dr}I_0\left(\frac{r}{\lambda}\right)}{I_1\left(\frac{b}{\lambda}\right)K_0\left(\frac{a}{\lambda}\right)+K_1\left(\frac{b}{\lambda}\right)I_0\left(\frac{a}{\lambda}\right)}\right]$. (S65)
It is known that $\frac{d}{dz}I_0(z) = I_1(z)$ and $\frac{d}{dz}K_0(z) = -K_1(z)$
Therefore the current of ligands at $r = a$ is
$J_r = -\frac{D_2\beta}{k_{endo}}\left[\frac{-I_1\left(\frac{b}{\lambda}\right)K_1\left(\frac{a}{\lambda}\right)+K_1\left(\frac{b}{\lambda}\right)I_1\left(\frac{a}{\lambda}\right)}{I_1\left(\frac{b}{\lambda}\right)K_0\left(\frac{a}{\lambda}\right)+K_1\left(\frac{b}{\lambda}\right)I_0\left(\frac{a}{\lambda}\right)}\right.$ (S66).

For the case $\frac{a}{\lambda} \ll 1$, we may exploit the asymptotic expansions corresponding to the modified Bessel functions for small arguments (18):
$K_0\left(\frac{a}{\lambda}\right) \sim -ln\left(\frac{a}{\lambda}\right)$ (S67),
$\frac{d}{dr}I_0\left(\frac{r}{\lambda}\right)(r = a) \sim 0$ (S68).
Therefore,
$J_r = -\frac{D_2\beta}{k_{endo}}\frac{I_1\left(\frac{b}{\lambda}\right)\left(\frac{1}{a}\right)}{I_1\left(\frac{b}{\lambda}\right)\left(\ln\left(\frac{a}{\lambda}\right)\right)} = -\frac{D_2\beta}{k_{endo}}\frac{1}{a\ln\left(\frac{a}{\lambda}\right)} = \frac{D_2\beta}{k_{endo}}\frac{1}{a\ln\left(\frac{\lambda}{a}\right)}$ (S69).
Hence

$N = \frac{D_2\beta}{k_{endo}}\frac{2\pi a\tau}{a\ln\left(\frac{\lambda}{a}\right)} = \frac{D_2\beta}{k_{endo}}\frac{2\pi\tau}{\ln\left(\frac{\lambda}{a}\right)}$ (S70).

The uncertainty is given by

$\left(\frac{\delta c}{\bar{c}}\right)^2 = \frac{1}{\langle N\rangle} = \frac{k_{endo}}{2\pi\tau D_2\beta}\ln\left(\frac{\lambda}{a}\right)$ (S71).

Since at steady state far away from the absorber $\bar{c} = \frac{\beta}{k_{endo}}$, we finally get:

$\left(\frac{\delta c}{\bar{c}}\right)^2 = \frac{1}{\langle N \rangle} = \frac{1}{2\pi\tau D_2 \bar{c}} \ln\left(\frac{\lambda}{a}\right)$ (S72),
which is a factor of 2 smaller than our result with 'perfect monitoring disk' approximation (Eq. S21).

Accuracy of ligand concentration measurement by one receptor using the FDT

We conclude the supplementary methods with an alternative computation of the accuracy in measuring ligand concentration. We analyze the effects of intrinsic fluctuations of the receptor-ligand system with the help of the fluctuation dissipation theorem (1,2)**.** First we calculate the accuracy in ligand concentration measurement due to binding to a single fixed receptor. Afterwards we extend the calculation to include the possibility of binding to several fixed receptors. We arrived to the same accuracy due to diffusion noise we obtained when we considered a perfect receptor with extrinsic noise in the receptor-ligand system.

We define *n(t)* as the occupation probability of one receptor bound to a ligand at position x_0 on the membrane of the receptor cell. The ligand concentration on the membrane of the ligand cell is described by $c(\boldsymbol{x}, t)$. We also assume that ligands are continuously recycled in and out of the membrane (e.g. through endocytosis and exocytosis with rates k_{endo} and k_{exo}, respectively. The dynamics of ligand-receptor is governed by

$$\frac{dn(t)}{dt} = k_+ c(\boldsymbol{x}, t)\big(1 - n(t)\big) - k_- n(t), \qquad \text{(S73)}$$

$$\frac{\partial c(\boldsymbol{x},t)}{\partial t} = D_2 \nabla^2 c(\boldsymbol{x}, t) - \delta(\boldsymbol{x} - \boldsymbol{x_0}) \frac{dn(t)}{dt} - k_{endo} c(\boldsymbol{x}, t) + k_{exo} c_{cyto}\,. \qquad \text{(S74)}$$

where D_2 is the 2D diffusion coefficient for the ligands on the cell membrane, k_+ and $k_-$are the binding and unbinding rates of the ligand-receptor complex, $\delta(\boldsymbol{x})$ is the Dirac delta function, and c_{cyto} is the concentration of a cytoplasmic pool of the Delta ligand (assumed to be constant in this study).

The rate constants obey the detailed balance equation:

$$\frac{k_+ \bar{c}}{k_-} = \exp\left(\frac{F}{kT}\right), \qquad \text{(S75)}$$

where F is the difference in the free energies between unbound and bound states of the receptor. We introduce small perturbations around the stationary solutions. The perturbations are defined according to the following

$$k_\pm = \overline{k_\pm} + \delta k_\pm,\ n = \bar{n} + \delta n, c = \bar{c} + \delta c,\ F = \bar{F} + \delta F. \qquad \text{(S76)}$$

The bar over the variables denotes steady state equilibrium values.

Substituting Eq. S76 into Eq. S75 leads to

$$\frac{\delta k_+}{k_+} - \frac{\delta k_-}{k_-} = \frac{\delta F}{k_B T}\,. \qquad \text{(S77)}$$

By substituting Eq. S77 into Eq. S73 we obtain that the perturbation δn satisfies

$$\frac{d\delta n(t)}{dt} = -\left(\bar{k}_+\bar{c} + \bar{k}_-\right)\delta n(t) + \bar{c}(1-\bar{n})\delta k_+ + \bar{k}_+\delta c(1-\bar{n}) - \bar{n}\delta k_-\,. \qquad \text{(S78)}$$

The perturbations of the rate constants $\delta k_\pm$ are connected by the Eq. S77, hence Eq. S78 becomes

$$\frac{kT}{\bar{k}_+\bar{c}(1-\bar{n})}\frac{d\delta n}{dt} + \frac{kT(\bar{k}_+\bar{c}+\bar{k}_-)}{\bar{k}_+\bar{c}(1-\bar{n})}\,\delta n(t) - kT\frac{\delta c}{\bar{c}} = \delta F\,. \qquad \text{(S79)}$$

In a similar way, Eq. S74 may be rewritten in terms of the perturbations δc and δn as follows

$$\frac{\partial \delta c(\boldsymbol{x},t)}{\partial t} = D_2\nabla^2\delta c(\boldsymbol{x},t) - \delta(\boldsymbol{x}-\boldsymbol{x_0})\frac{d\delta n(t)}{dt} - k_{endo}\delta c(\boldsymbol{x},t). \qquad \text{(S80)}$$

Fourier transform in spatial and temporal variables are defined as in Eq. S4.

The Fourier transform of Eq. S79 in the temporal variable is

$$\delta n(\omega)\left[-\frac{kT(i\omega)}{\bar{k}_+\bar{c}(1-\bar{n})} + \frac{kT(\bar{k}_+\bar{c}+\bar{k}_-)}{\bar{k}_+\bar{c}(1-\bar{n})}\right] - \frac{kT}{\bar{c}}\delta c = \delta F\,. \qquad \text{(S81)}$$

The Fourier transform in spatial and temporal variables of Eq. S80 becomes:

$$\delta c(\boldsymbol{k},\omega) = i\omega\frac{e^{-i\boldsymbol{k}\cdot x_0}\delta n(\omega)}{[-i\omega + D_2k^2 + k_{endo}]}\,. \qquad \text{(S82)}$$

The inverse Fourier transform in 2D is defined by

$$\delta c(\boldsymbol{x},\omega) = \frac{1}{(2\pi)^2}\int d^2k\; e^{i\boldsymbol{k}\cdot\boldsymbol{x}}\delta c(\boldsymbol{k},\omega). \qquad \text{(S83)}$$

Applying the inverse Fourier transform to Eq. S82 we obtain:

$$\delta c(\boldsymbol{x_0},\omega) = \frac{i\omega}{(2\pi)^2}\int d^2k\;\frac{\delta n(\omega)}{[-i\omega + D_2k^2 + k_{endo}]}. \qquad \text{(S84)}$$

Substituting Eq. S84 into the Eq. S81 we get:

$$\delta n(\omega)\left[-\frac{kT(i\omega)}{\bar{k}_+\bar{c}(1-\bar{n})} + \frac{kT(\bar{k}_+\bar{c}+\bar{k}_-)}{\bar{k}_+\bar{c}(1-\bar{n})} - \frac{kT}{\bar{c}}\frac{i\omega}{(2\pi)^2}\int d^2k\;\frac{1}{[-i\omega + D_2k^2 + k_{endo}]}\right] = \delta F. \qquad \text{(S85)}$$

We define the linear response function or the generalized susceptibility α by (2)

$$\alpha = \frac{\delta n(\omega)}{\delta F(\omega)}. \qquad \text{(S86)}$$

The generalized susceptibility in our particular case turns out to be

$$\alpha = \frac{\bar{k}_+\bar{c}(1-\bar{n})}{kT}\frac{1}{-i\omega\left[1+\bar{k}_+(1-\bar{n})\int\frac{d^2k}{(2\pi)^2}\frac{1}{[-i\omega+D_2k^2+k_{endo}]}\right]+(\bar{k}_+\bar{c}+\bar{k}_-)}. \quad \text{(S87)}$$

Defining

$$\sum(\omega) = \bar{k}_+(1-\bar{n})\int\frac{d^2k}{(2\pi)^2}\frac{1}{[-i\omega+D_2k^2+k_{endo}]}, \quad \text{(S88)}$$

we rewrite Eq. S87 as

$$\alpha = \frac{\bar{k}_+\bar{c}(1-\bar{n})}{kT}\frac{1}{-i\omega[1+\sum(\omega)]+(\bar{k}_+\bar{c}+\bar{k}_-)}. \quad \text{(S89)}$$

Since we are averaging over a time τ large compared to the noise correlation time $\tau_c = \left(\bar{k}_+\bar{c}+\bar{k}_-\right)^{-1}$, we need to take into consideration only the low frequency limit of the noise spectrum.

Eq. S88 diverges for large k. In order to regularize Eq. S88, we introduce a cut off for large k. This is equivalent to assume that the receptor has a finite size (2). Introducing polar coordinates $d^2k = kd\theta dk$, Eq. S88 can be rewritten as:

$$\sum(\omega\sim 0) = \bar{k}_+(1-\bar{n})\int\frac{d^2k}{(2\pi)^2}\frac{1}{D_2k^2+k_{endo}} =$$
$$\frac{\bar{k}_+(1-\bar{n})2\pi}{2(2\pi)^2D_2}[\ln(D_2k^2+k_{endo})]_0^{\frac{1}{a}} = \frac{\bar{k}_+(1-\bar{n})}{2\pi D_2}\ln\left(\frac{D_2}{a^2k_{endo}}+1\right)^{1/2} \approx \frac{\bar{k}_+(1-\bar{n})}{2\pi D_2}\ln\left(\frac{\lambda}{a}\right), \quad \text{(S90)}$$

with

$$\lambda \equiv \sqrt{\frac{D_2}{k_{endo}}}, \quad \text{(S91)}$$

as previously defined. For the derivation of Eq. S90 it was assumed $\lambda \gg a$, where a is the radius of the receptor.

The power spectrum or spectral density of a random variable $y(t)$ is defined as

$$S_y(\omega) = \lim_{T\to\infty}\frac{2}{T}\left|\int_{-T/2}^{T/2}[y(t)-\bar{y}]e^{i\omega t}\right|^2, \quad \text{(S92)}$$

and it satisfies

$$\int\frac{d\omega}{2\pi}S_y(\omega) = \lim_{T\to\infty}\frac{1}{T}\int_{-T/2}^{T/2}[y(t)-\bar{y}]^2 = \langle(\delta y)^2\rangle. \quad \text{(S93)}$$

In particular, the power spectrum $S_n(\omega)$ in occupancy may be defined by

$$\langle\delta n(\omega)\delta n(\omega')\rangle = 2\pi\delta(\omega+\omega')S_n(\omega). \quad \text{(S94)}$$

The Fluctuation Dissipation theorem connects the generalized susceptibility $\alpha(\omega)$ with the power spectrum $S_n(\omega)$ (2) by the relation $S_n(\omega) = \frac{2kT}{\omega} Im$ (α(ω)). Here we compute $S_n(\omega)$ and obtain

$$S_n(\omega) = \frac{2\bar{k}_+\bar{c}(1-\bar{n})[1+\sum(0)]}{\omega^2[1+\sum(0)]^2+\left((\bar{k}_+\bar{c}+\bar{k}_-)\right)^2}. \qquad \text{(S95)}$$

Using Eq. S90, the power spectrum $S_n(\omega)$ in occupancy can be rewritten as

$$S_n(\omega\sim 0) = \frac{2\bar{k}_+\bar{c}(1-\bar{n})[1+\sum(0)]}{(\bar{k}_+\bar{c}+\bar{k}_-)^2} = \frac{2\bar{n}(1-\bar{n})}{(\bar{k}_+\bar{c}+\bar{k}_-)} + \frac{\bar{n}^2(1-\bar{n})^2}{\pi D_2\bar{c}} \ln\left(\frac{\lambda}{a}\right). \qquad \text{(S96)}$$

Averaging over a time τ, the accuracy δn will take into account only low frequencies $|\omega| < \frac{1}{\tau_{int}}$:

$$\langle(\delta n)^2\rangle \sim \int_0^{|\omega|<\frac{1}{\tau}} \frac{d\omega}{2\pi} S_n(\omega) \sim \int_0^{|\omega|<\frac{1}{\tau}} \frac{d\omega}{2\pi} S_n(\omega\sim 0) = S_n(\omega\sim 0)\frac{\omega}{2\pi} = \frac{S_n(\omega\sim 0)}{\tau}. \text{ (S97)}$$

Therefore,

$$\delta n = \sqrt{S_n(0)/\tau}. \qquad \text{(S98)}$$

Finally using Eq. S96 we obtain that

$$\delta n > \frac{\bar{n}(1-\bar{n})}{\sqrt{\pi D_2\bar{c}\tau}} \sqrt{\ln\left(\frac{\lambda}{a}\right)}. \qquad \text{(S99)}$$

We may relate δc with δn using spectral densities of fluctuations. The power spectrum $S_c(\omega)$ satisfies,

$$\langle\delta c(t)\delta c(t')\rangle = \int \frac{d\omega}{2\pi} S_c(\omega)\, e^{-i\omega(t-t')}. \qquad \text{(S100)}$$

A total variation in the concentration *c* is equivalent to a variation in the chemical potential μ. Since $\frac{\Delta c}{\bar{c}} = \frac{\Delta F}{k_B T}$, we will have

$$S_c(\omega) = \left(\frac{\bar{c}}{k_B T}\right)^2 S_F(\omega). \qquad \text{(S101)}$$

The spectral density for F satisfies

$$S_n(\omega) = \alpha^2 S_F(\omega); \qquad \text{(S102)}$$

therefore

$$S_F(\omega) = \frac{2k_B T}{\omega\left|\frac{\delta\hat{n}}{\delta\hat{F}}\right|^2} Im\left[\frac{\delta\hat{n}}{\delta\hat{F}}\right], \qquad \text{(S103)}$$

which is equivalent to

$$S_F(\omega) = \frac{-2k_BT}{\omega} Im[\frac{\delta \hat{F}}{\delta \hat{n}}] \,. \qquad \text{(S104)}$$

Similarly to δn, the accuracy δc satisfies:

$$\delta c = \sqrt{S_c(\omega \sim 0)/\tau}. \qquad \text{(S105)}$$

Combining Eq. S105, Eq. S104, Eq. S101 and Eq. S99 we obtain

$$\frac{\delta c}{\bar{c}} > \frac{1}{\sqrt{\pi D_2 \bar{c} \tau}} \sqrt{\ln\left(\frac{\lambda}{a}\right)} \,. \qquad \text{(S106)}$$

Length scale in the absence of endocytosis

Now we proceed to show that endocytosis is not required in order to deal with the IR divergence in the zero frequency limit. If we neglect endocytosis, the diffusion length scale is replaced by $\sqrt{D_2\tau}$. In order to prove that, we rewrite Eq. S88 as

$$\sum(\omega) = \bar{k}_+(1-\bar{n}) \int \frac{d^2k}{(2\pi)^2} \frac{1}{[-i\omega + D_2k^2]} = \frac{\bar{k}_+(1-\bar{n})}{2\pi(2D_2)} [\ln(D_2k^2 - i\omega)]_0^{\frac{1}{a}} =$$

$$\frac{\bar{k}_+(1-\bar{n})}{2\pi(2D_2)} \left[\ln\left(\frac{D_2}{a^2} - i\omega\right) - \ln(-i\omega)\right]. \qquad \text{(S107)}$$

The log of a complex number $z = re^{i\theta}$ is defined by

$$\ln(z) = \ln(r) + i\theta. \qquad \text{(S108)}$$

Therefore

$$\sum(\omega) = \frac{\bar{k}_+(1-\bar{n})}{2\pi(2D_2)} [\frac{1}{2}\ln(\left(\frac{D_2}{a^2}\right)^2 + \omega^2) + i\theta_1 - \ln(\omega) - i\theta_2] = \sum_{real} + i\sum_{imaginary} \,, \qquad \text{(S109)}$$

θ_1 is the argument of the complex number $\frac{D_2}{a^2} - i\omega$ and $\theta_2 = \frac{3\pi}{2}$.

The generalized susceptibility is given by

$$\alpha = \frac{\bar{k}_+\bar{c}(1-\bar{n})}{kT} \frac{1}{-i\omega[1+\sum(\omega)] + (\bar{k}_+\bar{c} + \bar{k}_-)} \,. \qquad \text{(S110)}$$

The power spectrum $S_n(\omega)$ is

$$S_n(\omega) = \frac{2kT}{\omega} Im\,(\alpha(\omega)) = \frac{2\bar{k}_+\bar{c}(1-\bar{n})[1+\sum(\omega)_{real}]}{\omega^2[1+\sum(\omega)_{real}]^2 + \left((\bar{k}_+\bar{c} + \bar{k}_-) + \omega\sum_{imaginary}\right)^2} \,. \qquad \text{(S111)}$$

The IR divergence is contained solely in the term $\ln(\omega)$ in the zero frequency limit. The other terms containing ω are well behaved for small ω and can be set to 0 in the evaluation of $\langle(\delta n)^2\rangle \sim \int_0^{|\omega|<\frac{1}{\tau}} \frac{d\omega}{2\pi} S_n(\omega)$. The imaginary part $\omega\sum_{imaginary}$ disappears in the zero frequency limit.

We set $\omega \sim 0$ in all the terms that do not have IR divergence (i.e. except in the term involving $\ln(\omega)$).

Averaging over a time τ, for frequencies satisfying $|\omega| < \frac{1}{\tau_{int}}$ we obtain

$$\langle(\delta n)^2\rangle \sim \int_0^{|\omega|<\frac{1}{\tau}} \frac{d\omega}{2\pi} S_n(\omega) \sim \frac{2\bar{k}_+\bar{c}(1-\bar{n})}{(\bar{k}_+\bar{c}+\bar{k}_-)^2} \int_0^{|\omega|<\frac{1}{\tau}} \frac{d\omega}{2\pi} \frac{\bar{k}_+(1-\bar{n})}{2\pi(2D_2)} [(1 + \ln(\frac{D_2}{a^2})^2 - \ln\left(\frac{1}{\tau}\right)]$$

$$= \frac{2\bar{k}_+\bar{c}(1-\bar{n})}{(\bar{k}_+\bar{c}+\bar{k}_-)^2} \frac{\bar{k}_+(1-\bar{n})}{2\pi(2D_2)} \{[1 + 2\ln\left(\frac{D_2}{a^2}\right) + \ln(\tau)]\left(\frac{1}{\tau}\right) = \frac{2\bar{k}_+\bar{c}(1-\bar{n})}{(\bar{k}_+\bar{c}+\bar{k}_-)^2} \frac{\bar{k}_+(1-\bar{n})}{2\pi(2D_2)} \frac{2}{\tau}[\ln\left(\frac{D_2\tau}{a^2}\right)] = \frac{(\bar{n}(1-\bar{n}))^2}{\pi D_2 \bar{c}\tau} \ln\left(\frac{\sqrt{D_2\tau}}{a}\right).$$

(S112)

Here, we note we may define a new length scale

$$\lambda = \sqrt{D_2\tau}\,. \qquad \text{(S113)}$$

From here following the same computation we did for k_{endo} (see Eqs. S100-S106) we may obtain a similar expression to Eq. S26: $\frac{\delta c}{\bar{c}} > \frac{1}{\sqrt{\pi D_2 \bar{c}\tau}} \sqrt{\ln\left(\frac{\lambda^*}{a}\right)}$ with the length scale $\lambda^* = \sqrt{D_2\tau}$.

Accuracy of ligand concentration measurement by multiple receptors using the FDT

The extended equations for ligand and multiple molecule receptors become

$$\frac{dn_\mu(t)}{dt} = k_+ c(\boldsymbol{x_\mu}, \mathrm{t})\left(1 - n_\mu(t)\right) - k_- n_\mu(t), \qquad \text{(S114)}$$

$$\frac{\partial c(\boldsymbol{x},t)}{\partial t} = D_2\nabla^2 c(\boldsymbol{x},t) - \sum_{\mu=1}^{m} \delta(\boldsymbol{x} - \boldsymbol{x_\mu}) \frac{dn_\mu(t)}{dt} - k_{endo} c(\boldsymbol{x},t) + k_{exo} c_{cyto}. \qquad \text{(S115)}$$

As in the case of a single receptor, detailed balance requires Eq. S75.

Similarly to the case of one receptor, we introduce small perturbations around the stationary solutions:

$$k_\pm = \overline{k_\pm} + \delta k_\pm,\ n_\mu = \overline{n_\mu} + \delta n_\mu,\ c = \bar{c} + \delta c,\ F = \bar{F} + \delta F. \qquad \text{(S116)}$$

The rate constants $\delta k_\pm$ obey Eq. S77.

Substituting Eq. S116 into Eq. S114 we obtain

$$\frac{d\delta n_\mu}{dt} = -\left(\bar{k}_+\bar{c} + \bar{k}_-\right)\delta n_\mu(t) + \bar{c}\left(1-\overline{n_\mu}\right)\delta k_+ - \overline{n_\mu}\delta k_- + \bar{k}_+\delta c\left(1-\overline{n_\mu}\right). \quad \text{(S117)}$$

With the help of Eq. S77 we rewrite Eq. S117 as

$$\frac{kT}{\bar{k}_+\bar{c}\left(1-\overline{n_\mu}\right)}\frac{d\delta n_\mu}{dt} + \frac{kT(\bar{k}_+\bar{c}+\bar{k}_-)}{\bar{k}_+\bar{c}\left(1-\overline{n_\mu}\right)}\,\delta n_\mu(t) - k_BT\frac{\delta c}{\bar{c}} = \delta F. \qquad \text{(S118)}$$

We proceed to rewrite the ligand equation for the perturbation δc in terms of the corresponding Fourier transforms of δc and δn_μ (similar to the computation that lead to Eq. S82)

$$-i\omega\delta c(\boldsymbol{k},\omega) = \\ (-D_2k^2 - k_{endo})\delta c(\boldsymbol{k},\omega) + \iint d^2x\, dt \sum_{\mu=1}^{m}\delta\left(\boldsymbol{x}-\boldsymbol{x_\mu}\right)(i\omega)\delta n_\mu(\mathrm{t})e^{i(-\boldsymbol{k}\cdot\boldsymbol{x}+w\mathrm{t})}.$$

(S119)

Therefore,

$$\delta c\,(\boldsymbol{x},\omega) = \frac{1}{(2\pi)^2}(i\omega)\sum_{\mu=1}^{m}\int\frac{d^2k\;\delta n_\mu(\omega)}{[-i\omega+D_2k^2+k_{endo}]}e^{ik(-\boldsymbol{x_\mu}+\boldsymbol{x_\nu})}. \qquad \text{(S120)}$$

The integral appearing in Eq. S120 can be split into two cases (similar to the treatment of the 3D case by (2), namely μ=ν and μ≠ν.

The term corresponding to μ=ν is equal to

$$\delta c\,(\boldsymbol{x_\nu},\omega) = \delta n_\nu(\omega)(i\omega)\int\frac{1}{(2\pi)^2}\frac{d^2k}{[-i\omega+D_2k^2+k_{endo}]}, \qquad \text{(S121)}$$

which can be evaluated explicitly (the same integral was evaluated in Eq. S100)

$$\delta c\,(\boldsymbol{x_\nu},\omega) = \delta n_\nu(\omega)(i\omega)\frac{\ln\sqrt{\left(\frac{D_2}{a^2k_{endo}}+1\right)}}{2\pi D_2}. \qquad \text{(S122)}$$

The term corresponding to μ≠ν:

$$\delta c\,(\boldsymbol{x_\nu},\omega{\sim}0,\mu\neq\nu) = \frac{1}{(2\pi)^2D_2}(i\omega)\sum_{(\mu\neq\nu)=1}^{m}\int\frac{d^2k\;\delta n_\mu(\omega)}{\left[-\frac{i\omega}{D_2}+k^2+\frac{k_{endo}}{D_2}\right]}e^{i\boldsymbol{k}\cdot(-\boldsymbol{x}_\mu+\boldsymbol{x_\nu})}. \quad \text{(S123)}$$

The integral term appearing in Eq. S116 (for $\omega{\sim}0$) is the 2D inverse Fourier transform of the generalized function $\frac{1}{\left[k^2+\frac{k_{endo}}{D_2}\right]}$. This was computed already (Eqs.S30-S34).

Therefore, Eq. S116 can be rewritten as

$$\delta c\,(\boldsymbol{x_\nu}, \omega{\sim}0, \mu \neq \nu) = \frac{1}{(2\pi)^2 D_2}(i\omega)\sum_{(\mu\neq\nu)=1}^{m}\delta n_\mu(\omega)(2\pi)K_0\left(\sqrt{\frac{k_d}{D_2}}\left|\boldsymbol{x_\mu}-\boldsymbol{x_\nu}\right|\right).\ (S124)$$

This can be expressed in terms of the diffusion length λ (Eq. S84)

$$\delta c\,(\boldsymbol{x_\nu}, \omega{\sim}0, \mu \neq \nu) = \frac{1}{(2\pi)^2 D_2}(i\omega)\sum_{(\mu\neq\nu)=1}^{m}\delta n_\mu(\omega)(2\pi)K_0\left(\frac{\left|(x_\mu-\boldsymbol{x_\nu}\right|}{\lambda}\right). \quad (S125)$$

Now, the Fourier transform of Eq. S118 is

$$\text{-}i\omega\delta n_\mu = k_+\bar{c_\mu}\left(1-\overline{n_\mu}\right)\frac{\delta F(\omega)}{kT} + k_+\left(1-\overline{n_\mu}\right)\delta c\left(x_\mu,\omega\right) - \left(\overline{k_+}\bar{c_\mu} + \overline{k_-}\right)\delta n_\mu. \quad (S126)$$

Substituting Eq. S122 and Eq. S123 into Eq. S126 and summing over all receptors, we obtain

$$-i\omega\delta N(\omega) = -\left[(k_+\bar{c}+k_-) - (i\omega)k_+(1-\bar{n})\frac{\ln\sqrt{\left(\frac{D_2}{a^2k_{endo}}+1\right)}}{2\pi D_2}\right]\delta N + k_+(1-$$

$$\bar{n})\frac{(i\omega)}{(2\pi)^2 D_2}\sum_{\nu=1}^{m}\sum_{\mu\neq\nu}\delta n_\mu(\omega)\ K_0(\left|(\boldsymbol{x_\mu}-\boldsymbol{x_\nu})\right|/\lambda)(2\pi) + mk_+(1-\bar{n})\bar{c}\frac{\delta F(\omega)}{kT}.\ (S127)$$

Then,

$$-i\omega\delta N(\omega) =$$

$$-\left[\left(\overline{k_+}\,\bar{c}+\overline{k_-}\right) - (i\omega)\overline{k_+}(1-\bar{n})\frac{\ln\left(\frac{\lambda}{a}\right)}{2\pi D_2}\right]\delta N +$$

$$\overline{k_+}(1-\bar{n})\frac{(i\omega)}{2\pi D_2}\sum_{\nu=1}^{m}\sum_{\mu\neq\nu}\delta n_\mu(\omega)\ K_0(\left|(\boldsymbol{x_\mu}-\boldsymbol{x_\nu})\right|/\lambda) + m\overline{k_+}(1-\bar{n})\bar{c}\frac{\delta F(\omega)}{kT}.\ (S128)$$

Here we added over all receptors and defined the total occupancy of the receptor cluster as $\delta N(\omega) = \sum_{\mu=1}^{m}\delta n_\mu$.

In cases where the inner sum is independent of x_ν (like in the symmetries contemplated in (2)) we rewrite the sum as

$$\sum_{\nu=1}^{m}\sum_{\mu\neq\nu}\delta n_\mu(\omega)\ K_0\left(\frac{\left|(\boldsymbol{x_\mu}-\boldsymbol{x_\nu}\right|}{\lambda}\right) = \delta N(\omega)\sum_{\mu=2}K_0\left(\frac{\left|(x_\mu-x_1\right|}{\lambda}\right). \quad (S129)$$

For the sake of simplicity, we will assume a cluster of m receptors of size *a* distributed equidistantly along a ring of radius *s* (Eqs. S36-S37). This assumption allows us to simplify Eq. S129.

Then following a similar procedure to the one used to calculate the accuracy of ligand concentration measurement by one receptor, we obtain

$$S_F(\omega{\sim}0) = -2k_BT[-\frac{\ln\left(\frac{\lambda}{a}\right)}{2\pi\bar{c}mD_2} - \frac{1}{\overline{k_+}(1-\bar{n})m\bar{c}} - \frac{\sum_{i=1}^{m-1}K_0\left(\frac{2s}{\lambda}\sin\left(\frac{\pi i}{m}\right)\right)}{2\pi\bar{c}mD_2}]. \quad (S130)$$

So, using Eq. S111 and Eq. S129 we obtain

$$S_c(\omega\sim 0) = 2\bar{c}\left[\frac{\ln(\frac{\lambda}{a})}{2\pi m D_2} + \frac{1}{k_+(1-\bar{n})m} + \frac{\sum_{i=1}^{m-1} K_0(\frac{2s}{\lambda}\sin(\frac{\pi i}{m}))}{2\pi m D_2}\right]. \qquad \text{(S131)}$$

And therefore

$$\left(\frac{\delta c}{\bar{c}}\right)^2 = \left[\frac{\ln(\frac{\lambda}{a})}{\pi m D_2 \bar{c}\tau} + \frac{2}{k_+(1-\bar{n})\tau m\bar{c}} + \frac{\sum_{i=1}^{m-1} K_0(\frac{2s}{\lambda}\sin(\frac{\pi i}{m}))}{\pi m D_2 \bar{c}\tau}\right], \qquad \text{(S132)}$$

Hence

$$\left(\frac{\delta c}{\bar{c}}\right) > \frac{1}{\sqrt{\pi D_2 \bar{c}\tau m}}\sqrt{\ln(\frac{\lambda}{a}) + \sum_{i=1}^{m-1} K_0\left(\frac{2s}{\lambda}\sin\left(\frac{\pi i}{m}\right)\right)}. \qquad \text{(S133)}$$

Eq. S133 is similar to Eq. S39. Then again for the limiting case $\frac{s}{\lambda} \ll 1$

we obtain the final expression

$$\frac{\delta c}{\bar{c}} > \frac{1}{\sqrt{\pi D_2 \bar{c}\tau}}\sqrt{\frac{\ln\left(\frac{\lambda}{ma}\right)}{m} + \left(\frac{m-1}{m}\right)\ln\left(1.1228\frac{\lambda}{s}\right)}, \qquad \text{(S134)}$$

(see Eq. S44).

Supporting References

1. Kubo, R. (1966).The fluctuation-dissipation theorem. Rep. Prog. Phys. 29, 255-284.
2. Bialek, W. and Setayeshgar, S. (2005). Physical limits to biochemical signaling. Proc. Natl. Acad. Sci. U.S.A. 102, 10040-10045.
3. Chaikin, P. M. and Lubensky T. C. (1995). Principles of condensed matter physics. Cambridge University Press.
4. Landau L. D. and Lifshitz E. M. (1980). Statistical Physics Part I. Pergamon Press.
5. Pathria, R. K. (1972). Statistical Mechanics. Pergamon Press.
6. Landau L. D. and Lifshitz E. M. (1980). Statistical Physics Part II. Pergamon Press.
7. Berg , H. C. and Purcell, E. M. (1977). Physics of Chemoreception. Biophys. J. 20, 193-219.
8. McCloskey MA & Poo MM (1986). Rates of membrane-associated reactions: reduction of dimensionality revisited. J Cell Biol 102(1):88-96.
9. Kusumi, A., Nakada, C., Ritchie, K., Murase, K., Suzuki, K., Murakoshi, H., Kasai, R.S., Kondo, J., and Fujiwara, T. (2005). Paradigm shift of the plasma membrane concept from the two-dimensional continuum fluid to the

partitioned fluid: high-speed single-molecule tracking of membrane molecules. Annu Rev Biophys Biomol Struct *34*, 351-378.

10. Wiley HS & Cunningham DD (1982). The endocytotic rate constant. A cellular parameter for quantitating receptor-mediated endocytosis. J Biol Chem 257(8):4222-4229.
11. Sorkin A & Duex JE (2010). Quantitative analysis of endocytosis and turnover of epidermal growth factor (EGF) and EGF receptor. *Curr Protoc Cell Biol* Chapter 15: Unit 15 14.
12. Felder, S., LaVin, J., Ullrich, A., and Schlessinger, J. (1992). Kinetics of binding, endocytosis, and recycling of EGF receptor mutants. J Cell Biol *117*, 203-212.
13. Cole, N.B., and Donaldson, J.G. (2012). Releasable SNAP-tag probes for studying endocytosis and recycling. ACS Chem Biol *7*, 464-469.Jacobson K, Ishihara A, & Inman R (1987).
14. Tkacik G & Bialek W (2009). Diffusion, dimensionality, and noise in transcriptional regulation. Phys Rev E Stat Nonlin Soft Matter Phys 79: 051901-1-051901-9.
15. Kanwal, Ram P. (1983). Generalized Functions Theory and Technique. Mathematics in Science and Engineering. Vol 171. Academic Press.
16. Gelfand, I. M. and Shilov, G. E. (1964). Generalized Functions. Vol 1. Properties and Operations. Academic Press.
17. Morse, P. M. and Feshbach H (1953). Methods of Theoretical Physics. Vol 1. McGraw-Hill Book company INC.
18. Olver, Frank W.J., Lozier, Daniel W., Boisvert, Ronald F., Clark, Charles W. (2010). NIST Handbook of Mathematical Functions. Cambridge University Press.
19. http://www.siam.org/journals/categories/05-001.php
20. Goldstein B., Griego R., Wofsy C. (1984). Diffusion-limited forward rate constants in two dimensions. Application to the trapping of cell surface receptors by coated pits. Biophys. J. 46, 573-586.
21. Endres R. G., Wingreen N. S. (2008). Accuracy of direct gradient sensing by single cells. Proc. Natl. Acad. Sci. U.S.A. 105, 15749-15754.